UPPSALA
UNIVERSITET

Digital Comprehensive Summaries of Uppsala Dissertations from the Faculty of Science and Technology 1527

Studies of the two redox active tyrosines in Photosystem II

NIGAR AHMADOVA

ACTA
UNIVERSITATIS
UPSALIENSIS
UPPSALA
2017

ISSN 1651-6214
ISBN 978-91-554-9933-4
urn:nbn:se:uu:diva-320916

Dissertation presented at Uppsala University to be publicly examined in Room 2001, Ångströmlaboratoriet, Lägerhyddsvägen 1, Uppsala, Wednesday, 14 June 2017 at 13:15 for the degree of Doctor of Philosophy. The examination will be conducted in English. Faculty examiner: Professor Robert Burnap (Oklahoma State University, USA).

Abstract

Ahmadova, N. 2017. Studies of the two redox active tyrosines in Photosystem II. *Digital Comprehensive Summaries of Uppsala Dissertations from the Faculty of Science and Technology* 1527. 72 pp. Uppsala: Acta Universitatis Upsaliensis. ISBN 978-91-554-9933-4.

Photosystem II is a unique enzyme which catalyzes light induced water oxidation. This process is driven by highly oxidizing ensemble of four Chl molecules, P_{D1}, P_{D2}, Chl_{D1} and Chl_{D2} called, P_{680}. Excitation of one of the Chls in P_{680} leads to the primary charge separation, $P_{680}^{+}Pheo^{-}$. $Pheo^{-}$ transfers electrons sequentially to the primary quinone acceptor Q_A and the secondary quinone acceptor Q_B. P_{680}^{+} in turn extracts electrons from Mn_4CaO_5 cluster, a site for the water oxidation. There are two redox active tyrosines, Tyr_Z and Tyr_D, found in PSII. They are symmetrically located on the D1 and D2 central proteins. Only Tyr_Z acts as intermediate electron carrier between P_{680} and Mn_4CaO_5 cluster, while Tyr_D does not participate in the linear electron flow and stays oxidized under light conditions. Both tyrosines are involved in PCET.

The reduced Tyr_D undergoes biphasic oxidation with the fast (msec-sec time range) and the slow (tens of seconds time range) kinetic phases. We assign these phases to two populations of PSII centers with proximal or distal water positions. We also suggest that the Tyr_D oxidation and stability is regulated by the new small lumenal protein subunit, PsbTn. The possible involvement of PsbTn protein in the proton translocation mechanism from Tyr_D is suggested.

To assess the possible localization of primary cation in P_{680} the formation of the triplet state of P_{680} and the oxidation of Tyr_Z and Tyr_D were followed under visible and far-red light. We proposed that far-red light induces the cation formation on Chl_{D1}.

Transmembrane interaction between Q_B and Tyr_Z has been studied. The different oxidation yield of Tyr_Z, measured as a S_1 split EPR signal was correlated to the conformational change of protein induced by the Q_B presence at the Q_B-site. The change is transferred via H-bonds to the corresponding His-residues via helix D of the D1 protein.

Keywords: Photosystem II, Tyrosine Z and D, proton-coupled electron transfer

Nigar Ahmadova, Department of Chemistry - Ångström, Molecular Biomimetics, Box 523, Uppsala University, SE-75120 Uppsala, Sweden.

ISSN 1651-6214
ISBN 978-91-554-9933-4
urn:nbn:se:uu:diva-320916 (http://urn.kb.se/resolve?urn=urn:nbn:se:uu:diva-320916)

To my parents for their endless love and support!

List of Papers

This thesis is based on the following papers, which are referred to in the text by their Roman numerals.

I Sjöholm, J., Ho, F.*, Ahmadova, N., Brinkert, K., Hammarström, L., Mamedov, F.*, Styring, S. (2016). The protonation state around TyrD/TyrD• in photosystem II is reflected in its biphasic oxidation kinetics. *Biochim. Biophys. Acta,* 1858(2):147-155

II Ahmadova, N., Ho, M.F., Styring, S., Mamedov, F.* (2017) Tyrosine D oxidation and redox equilibrium in Photosystem II. *Biochim. Biophys. Acta,* 1858(6):407-417

III Pavlou, A., Jacques, J., Ahmadova, N., Mamedov, F.*, Styring, S.* The triplet state of the primary donor, P_{680}, in Photosystem II is not formed by far-red light at 5 K; implications for the localization of the primary radical pair. *Manuscript*

IV Ahmadova, N., Mamedov, F.* Formation of tyrosine radicals in Photosystem II under far-red light illumination. *Submitted manuscript*

V Ahmadova, N., Schröder, P.W.*, Mamedov, F. Role of the PsbTn, a small luminal protein in Photosystem II, in the redox reactions of Tyrosine D. *Manuscript*

VI Ahmadova, N., Mamedov, F.* The donor-acceptor side interactions in Photosystem II. *Manuscript*

Contents

Introduction 11
Solar energy 11

Overview of Photosynthesis 13

Photosystem II: The biological machinery of water splitting 16
Protein constituents of Photosystem II 16
Redox-active cofactors of electron transfer chain 17
WOC – water oxidizing complex 20

Tyr_Z and Tyr_D: two redox active tyrosines in Photosystem II 22
Protein environment 22
Functional differences 23
Interaction of tyrosines with S-states of WOC 25

Methods 27
Electron Paramagnetic Resonance 27
Fluorescence 29
Thermoluminescence 30

The protonation state around $Tyr_D/Tyr_D^{\bullet}$ and redox equilibrium in Photosystem II 32

Far-red light triggered induction of P_{680}^{+} and tyrosine radicals formation ... 41

Role of the PsbTn subunit in steering H^+ from Tyr_D 46

The Donor-Acceptor side interactions in Photosystem II 50

Sammanfattning 51

Xülasə 57

Acknowledgements 61

References 64

Abbreviations

ATP	adenosine triphosphate
Car	β-carotene
Chl	chlorophyll
Cyt	cytochrome
DCBQ	2,5 dichloro-1,4-benzoquinone
DCMU	3-(3,4-dichlorophenyl)-1,1-dimethylurea
DMBQ	dimethyl 1,4-benzoquinone
DMSO	dimethyl sulfoxide
DQ	duroquinone
EPR	electron paramagnetic resonance
FNR	FAD-containing ferredoxin-NADP+ reductase
FTIR	Fourier transform infrared
HQ	hydroquinone
QM/MM	quantum mechanics/molecular mechanics
LHC	light harvesting complex
NADPH	nicotinamide adenine dinucleotide phosphate
P680	the reaction center chlorophyll
PCET	proton coupled electron transport
Pheo	pheophytin
PpBQ	phenyl p-benzoquinone
PQ	plastoquinone
PQ-10	decylplastoquinone
PSI	photosystem I
PSII	photosystem II
QA	primary quinone acceptor in photosystem II
QB	secondary quinone acceptor in photosystem II
TL	Thermoluminescence
WOC	water oxidizing complex
TyrD	tyrosine 160 on the D2 protein
TyrZ	tyrosine 161 on the D1 protein

Introduction

The biological machinery to efficiently capture, convert and store solar energy in the chemical bonds of energy-rich molecules was invented by nature more than 3 billion years ago [2, 3]. This process, called photosynthesis, led to the explosion of biological activity on Earth with an enormous diversity of living organisms. The accumulation of a large amount of biomass is an undeniable evidence of such event. The carbon stored in this biomass has provided us with fuels, food and other useful chemicals to maintain our everyday life.

Solar energy

Currently, the rate of global energy consumption is about 16.3 TW, 40 % of which used by the EU and the USA [4]. This value constantly rises owing to continuous industrialization and the increase of world population. It is projected to reach 20 TW or more by 2030, and more than double that by 2050 [5, 6]. At the present time, about 85 % of consumed global energy is derived from fossil fuels [4, 7]. The remaining 15 % is nuclear, hydroelectric, and renewable energy sources, such as wind, biomass, solar panels, etc. [4]. The availability of fossil fuels lead to the suppression of development non-fossil energy sources. Estimates of the global oil, gas and coal reserves indicate they are more than sufficient to meet energy demands for at least a century [8]. Therefore, the current problem in the global arena is not the future lack of fossil fuels but, rather the consequences of its usage [9]. If we burn all fossil fuel reserves, the total amount of CO_2 accumulated in the atmosphere and oceans will be equivalent to the level of CO_2 which existed before life appeared on Earth [10]. To tackle this problem, we have to develop new technologies based on principles that the energy source must be abundant, renewable, safe and clean. One such source available to us is solar radiation [11]. The solar energy reaching our planet annually is approximately 100 000 TW,

far exceeding our present energy demands. In other words, the solar energy absorbed by the earth during about 2 hours is equal approximately to the energy used by mankind in an entire year [12]. Nature has mastered the task of solar energy conversion by the process of photosynthesis [13]. The biomass produced annually during photosynthesis is estimated to be more than 100 billion tons of dry weight, which corresponds to about 100 TW of energy [12]. The success of this natural phenomenon, photosynthesis, on such a significant scale is due to the infinite amounts of raw materials and energy required to drive it, i.e. solar energy, water and carbon dioxide. The key of this process is the oxidation of water into oxygen, electrons and protons. The oxygen is released into the atmosphere and creates the living environment for all aerobic organisms. The electrons and protons extracted from water during photosynthesis are used to make energy rich molecules.

Our goal would be to make an artificial light-driven system that can convert solar energy into energy rich products. If we could succeed in mimicking photosynthesis in efficient artificial systems, it would assist in solving the energy demands of mankind. Artificial photosynthesis could provide fuels with high energy density such as hydrogen, methane etc., meanwhile significantly reducing the amount of CO_2 in the atmosphere [12]. The more we learn about natural photosynthesis the greater possibility we will have in achieving success in making biomimetic robust artificial systems.

Overview of Photosynthesis

Photosynthesis is a large-scale process of solar energy conversion into the energy rich chemical products in the biosphere [12]. Photosynthesis is carried out by both fundamental domains of life, bacteria and eukarya [14]. Bacterial photosynthesis, based on the released byproduct, is divided to two types: anoxygenic (non-oxygen evolving) and oxygenic (oxygen evolving). Oxygenic photosynthesis is performed by cyanobacteria along with eukaryotic organisms: plants and algae. O_2 as a byproduct of this process is released into the atmosphere to support aerobic life [14]. Oxygenic photosynthesis is a complex process that can be simplified to the following reaction:

$$6CO_2 + 6H_2O \xrightarrow{h\nu} 6(CH_2O) + 6O_2$$

This reaction of photosynthesis occurs within the photosynthetic cells in specialized organelles known as chloroplasts (Fig. 1). Chloroplasts are comprised of two envelope membrane systems: the outer membrane and the inner membrane. The fluid-filled space of the chloroplast is called stroma. Within the stroma there is a third membrane system called thylakoid membrane. The thylakoid membrane is a network of flattened disks arranged in stacks called grana which are interconnected by the stroma lamellae membranes. The inner part of thylakoid membrane is called lumen.

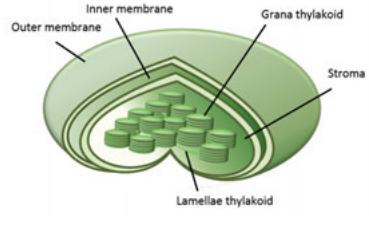

Figure 1. Structure of chloroplast

Photosynthesis consists of two sets of reactions: the light dependent and light independent reactions. In oxygenic photosynthetic organisms, the light dependent reactions are performed by the chain of three large protein supercomplexes embedded in the thylakoid membrane: Photosystem II (PSII), Cytochrome b_6f (Cyt b_6f) and Photosystem I (PSI) (Fig. 2).

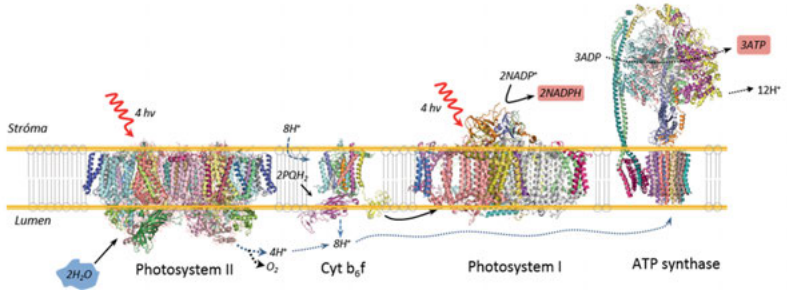

Figure 2. Photosynthetic electron transfer chain of the thylakoid membrane.

The electron transfers through these supercomplexes was first proposed by Hill and Bendal and implemented in the form of a Z-scheme by Duysens (Fig. 3) [15, 16].

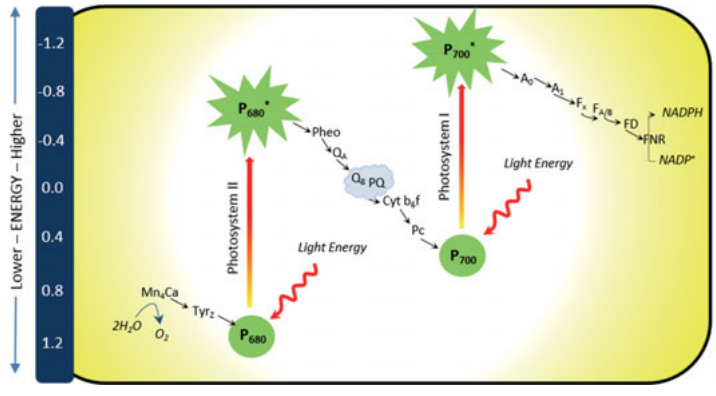

Figure 3. The Z-scheme of photosynthesis. The diagram indicates the major component of the light driven electron transport chain on an energy scale. The process is initiated by absorption of light by antenna complexes of the two photosystems, PSII and PSI.

The light reaction of photosynthesis is initiated in PSII. After the light absorption the reaction center chlorophyll of PSII loses an electron to an electron transport chain. The electron generated by PSII is replaced in the process of water splitting. The electrons leaving PSII are shuttled to PSI via Cyt b_6f complex. In PSI the low energy electrons are reenergized and pass through electron transfer cofactors of PSI to reduce Feredoxin (Fd) in the stroma. Fd in turn passes an electron to the FAD-containing ferredoxin-$NADP^+$ reductase (FNR) where the reduction of $NADP^+$ to NADPH takes place. As electrons pass through the electron transport

chain, their energy is used to translocate protons from stroma to lumen forming transmembrane proton gradient. The transmembrane proton gradient drives the protein complex called ATP synthase to generate ATP.

The light independent, or dark reactions, occur in the stroma of chloroplasts. These reactions are fueled by two molecules that are called the *energy currency* of the cells produced during the light reactions, NADPH and ATP. The dark reactions consist of several enzymatic steps collectively called Calvin-Benson-Bassham cycle to synthesize carbohydrates from CO_2. The carbon fixation reactions represent one of the nature´s most sustainable production lines.

Photosystem II: The biological machinery of water splitting

Photosystem II is a unique oxygen-evolving enzyme which catalyzes the water oxidation reaction in the thylakoid membranes of oxygenic organisms [17]. Nature had to fulfill two imperative functional goals to enable living organisms to split water by sun light: (i) formation of light-induced oxidizing cofactors that could be a driving force for water splitting and (ii) assembly of a catalytic site where water splitting could occur stepwise to store charges and prevent the generation of harmful intermediates. This chapter focuses on the overall structure of PSII and the electron transfer chain involved in oxidative water splitting in plants, algae and cyanobacteria.

Protein constituents of Photosystem II

PSII is a pigment-protein complex composed of more than 25 protein subunits, 105 chlorophylls, 28 carotenoids, chain of the redox cofactors and water oxidizing complex (WOC) per monomer [1]. Active PSII exists in a dimeric form located in the stacked regions of grana thylakoids (Fig. 4A) [1, 18, 19].

PSII dimer is 105x205x110 Å with a molecular mass of 700 kDa. The top view of PSII dimer surrounded by pigment-antenna complexes is depicted in Fig. 4B. The monomeric PSII core complex consists of four large intrinsic proteins (D1, D2, CP43 and CP47), twelve small membrane-spanning subunits (PsbE, PsbF, PsbH, PsbI, PsbJ, PsbK, PsbL, PsbM, PsbTc, PsbW, PsbX and PsbZ) and four extrinsic protein subunits (PsbO, PsbP, PsbQ and PsbTn) [1] . Most redox cofactors of PSII are housed by the D1 (psbA) and D2 (psbD) heterodimer. CP43 and CP47 are the inner light-harvesting antenna proteins of PSII, bind Chl_a and β-carotenes.

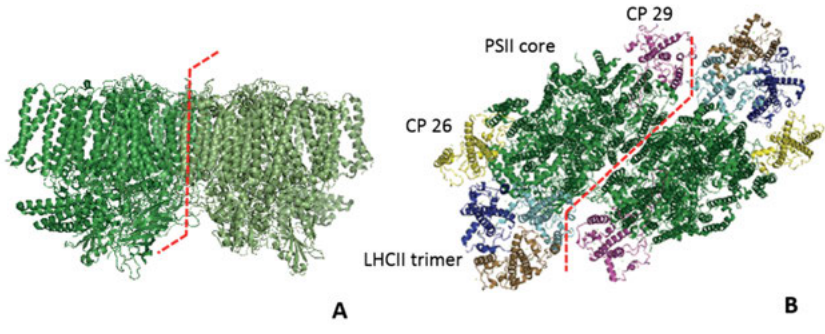

Figure 4. (A) Side view of the dimer of Photosystem II (PDB-4UB6, 1.9 Å resolution) colored by monomers. (B) Top view of spinach PSII–LHCII supercomplex (PDB-3JCU, 3.2 Å).

Apart from the inner antenna complex, each PSII dimer is surrounded by number of periferal light-harvesting antenna complexes, denoted CP29, CP26, CP24 and LHCII trimers. Contrary to CP43 and CP47, LHCII, CP24, CP26 and CP29 bind not only Chl_a but also Chl_b and xanthophylls (lutein, violaxanthin and neoxanthin). The other twelve low-molecular intrinsic subunits surround the PSII core. Only two of them (PsbE and PsbF) bind the cofactor of the electron transport chain, namely the heme group of cytochrome b_{559} (Cyt b_{559}) which plays an essential role in PSII assembly and protection against photodamage [20, 21]. However, the remaining small proteins were found to be an essential for assembly, stabilization and dimerization of the PSII core complexes (PsbH, PsbI, PsbJ, PsbK, PsbL, PsbM, PsbTc, PsbW, PsbX and PsbZ) [20].

The three extrinsic subunits, namely PsbO, PsbP, PsbQ cover WOC complex on the lumenal side. Their absence leads to the loss of water oxidation activity. The function of the forth extrinsic subunit, PsbTn was unknown at the time [1].

In addition to the above listed subunits, over 1300 water molecules were found in each PSII monomer, some directly interacting with WOC, as revealed in the 1.9 Å resolution structure from *T. vulcanus* [22].

Redox-active cofactors of electron transfer chain

The D1 and D2 heterodimer houses the redox-active components involved in the charge separation, water splitting and reduction of the terminal electron acceptor of PSII, plastoquinone Q_B. The electron transfer

chain of PSII is divided into the donor and acceptor side (Fig. 5) [18]. The oxidation of water occurs at the donor side of PSII. The acceptor side is a part of the electron transfer chain from P_{680} to the terminal electron acceptor, plastoquinone Q_B. The acceptor side cofactors are arranged around the pseudo-two-fold axis of transmembrane helices of D1 and D2 proteins. The axis passes through the middle of Chl dimer P_{D1} and P_{D2} to the non-heme Fe. The primary and secondary quinones, Q_A and Q_B are located on each side of the non-heme Fe on the D2 and D1 proteins respectively.

The light induced reaction starts from photoexcitation of antenna-pigment complexes (the peripheral and the inner antenna complexes) and exciton migration towards the reaction center Chls, P_{680}. P_{680} is the primary electron donor of PSII which consists of 4 chlorophyll molecules P_{D1}, P_{D2}, Chl_{D1} and Chl_{D2}. The P_{D1} and P_{D2} are positioned relatively close to each other forming a weak excitonic interaction between their tetrapyrolle head groups. After photoexcitation of one of the chlorophylls in P_{680}, the reaction center loses an electron to the nearby Pheo. Pheo is a chlorophyll molecule without a central Mg^{+2} ion in the porphyrin ring. The primary charge separation between P_{680} and $Pheo_{D1}$ is a very rapid process, happening in 3-4 psec. Reduced $Pheo_{D1}^-$ transfers an electron to the immobile primary quinone acceptor, Q_A in 300 psec [23]. All these steps are one electron transfer reaction. Q_A^- in turn transfers an electron to the secondary quinone acceptor, Q_B [17]. After two subsequent electron transfer reactions, Q_B gets protonated from the stromal side and leaves the Q_B site, making place for the new quinol molecule to bind. Q_BH_2 diffuses towards the binding site on the Cyt b_6f complex, and, upon binding, transfers electrons to Cyt b_6f and releases protons to the lumen, thus contributing to the transmembrane proton gradient. PSII is the only known protein complex in nature capable of splitting water. The driving force of this energetically challenging reaction is P_{680}^+. The primary donor P_{680}^+, has the highest oxidizing potential among any cofactors reported in biological systems, 1.25 eV [24, 25].

P_{680}^+ oxidizes a redox active tyrosine residue Tyr_Z (D1-Tyr161). Then, oxidized Tyr_Z extracts electrons stepwise from Mn_4CaO_5-cluster. The catalytic site of WOC, Mn_4CaO_5-cluster has to go through a series of five intermediate S_n-states (n = 0, 1, 2, 3, 4), called S (Kok) cycle to oxidize water to final product of the reaction, molecular O_2, by releasing four

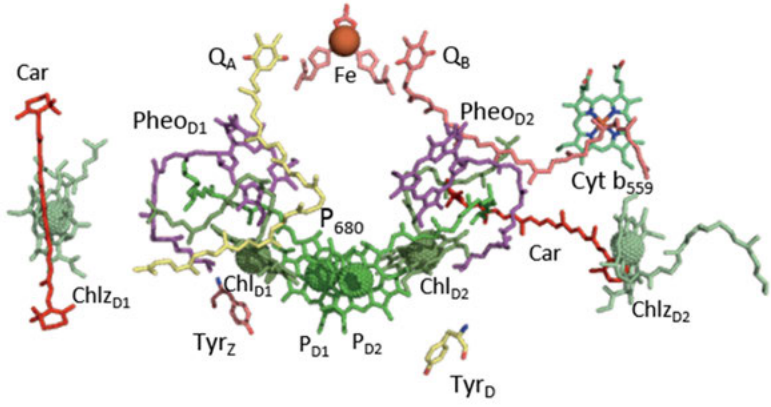

Figure 5. The redox active cofactors of PSII (PDB-4UB6, 1.9 Å resolution).

protons to the lumen and transferring four electrons via Tyr_Z to P_{680}^+ [26, 27].

PSII contains a second redox active tyrosine homologous to Tyr_Z on the D2 protein, denoted as Tyr_D (D2-Tyr160). Tyr_D is not involved in the linear electron transfer reaction from WOC and stays fully oxidized under the light.

The only redox component in PSII not bound by D1/D2 is cytochrome b_{559} (Cyt b_{559}) [28]. It is comprised of α and β subunits (PsbE and PsbF) coordinating the heme. Cyt b_{559} together with Chl_Z and β-carotene form a side electron pathway to P_{680}. Cyt b_{559} can also serve as acceptor of electrons from reduced Q_B. Cyt b_{559} is not a competitor with WOC due to the slow kinetics timescale, but serve as additional electron donors to P_{680} to protect the system during destructive high light conditions [29].

WOC – water oxidizing complex

The WOC is an inorganic cluster bound in the protein pocket of mostly D1 and also CP43 proteins on the luminal side of thylakoid membrane where water oxidation takes place [18]. It is composed of four Mn, one Ca and five oxygen atoms. Four oxygen atoms bridge among three Mn and one Ca atoms, forming an irregular cubical cluster, Mn_3CaO_4 which, in turn, connects to the fourth Mn (Mn4) via μ-oxos bridge (O4 and O5) (Fig. 6A).

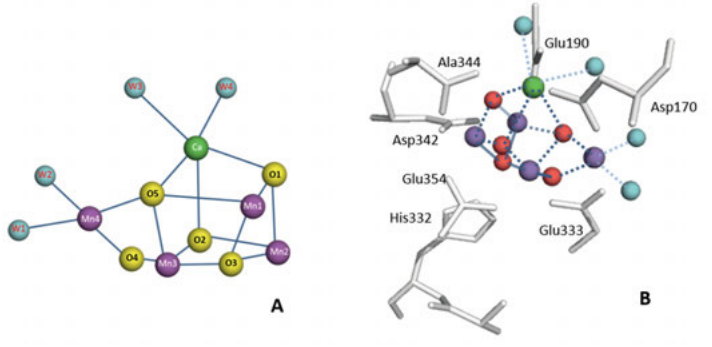

Figure 6. Structure (A) and protein environment (B) around the Mn_4CaO_5 cluster (PDB-4UB6, 1.9 Å resolution).

The shape of the whole cluster looks like a distorted chair, with the cubical part Mn_3CaO_4 serving as the chair base, and the fourth Mn (Mn4) as the back of the chair. According to the current knowledge based on a variety of spectroscopic techniques and calculations, the distorted chair shape of the cluster has an advantage during water splitting reaction, allowing structural rearrangements during the S-state cycle advancement.

In the dark stable S_1 state of a Mn_4CaO_5 cluster, four water molecules (W1-W4) were found directly ligated to the cluster [18]. W1 and W2 are associated with Mn4 and the other two W3 and W4 with the Ca atom. Since there were no other water molecules found ligated to the cluster, it was suggested that some of these water molecules serve as the substrate for the water splitting reaction [30].

The Mn_4CaO_5 cluster is coordinated by seven amino acids where six of them are carboxylate residues and only one is His (D1-His332) which ligated to Mn1 (Fig. 6A) [18, 31]. All of the carboxylate residues serve as bidentate ligands (D1-Asp170, D1-Glu333, D1-Asp342, D1-Ala344, and CP43-Glu354) except for D1-Glu189, which is a monodentate ligand

to Mn1. Together with water molecule and oxo-bridges, these amino acids bring about a saturating ligand environment for the Mn_4CaO_5 cluster, with six ligation to of the each manganese ions and seven to the calcium.

WOC must pass through five oxidation states, S_i, of so called Kok cycle, where *i* denotes the number of oxidizing equivalents stored after each charge separation in order to extract 4 electrons and 4 protons (H^+) and, finally, oxidize two molecules of water to O_2 (Fig. 7) [27, 32]. The S transitions of WOC represent single electron oxidation process, caused by reduction of P_{680}^+ through Tyr_Z. The Kok cycle starts with the most reduced S_0 state of the Mn_4CaO_5 cluster. Photon absorption by P_{680} drives S_0-S_1 transition. S_1 is the most stable state of Mn_4CaO_5 cluster in the dark and the dark-adapted PSII centers, the cluster is found mostly in the S_1 state (75 %) [33-35]. Subsequent photon absorptions lead to the S_1-S_2, S_2-S_3 and S_3-S_4 transitions where O_2 is released. S_4 is a transient state that has not yet been detected [26].

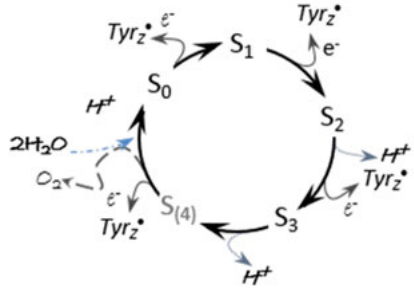

Figure 7. The S-state cycle of WOC

Tyr_Z and Tyr_D: two redox active tyrosines in Photosystem II

Tyrosyl radicals play crucial role in the oxidative reactions of many enzymes. One such enzyme is Photosystem II. There are two redox active tyrosines, Tyr_Z and Tyr_D, involved in light-induced electron transfer reactions [36]. By site-directed mutagenesis it was shown that Tyr_Z is tyrosine 161 of the D1 protein, and Tyr_D is tyrosine 160 of the D2 protein [37]. Both redox active tyrosines are symmetrically positioned in the D1 and D2 proteins respectively. However, only one of them, namely Tyr_Z, is directly involved in the water oxidation [3]. The other redox active tyrosine, Tyr_D, is in slow redox equilibrium with the WOC but can also be oxidized by P_{680}^+ at certain conditions [38]. The structural and functional difference between the two redox active tyrosines, as well as the redox reactions involving them, will be discussed in this chapter.

Protein environment

Tyr_Z (Tyr-161) is located in the D1 protein between the Mn_4CaO_5 cluster and P_{680}. As it was confirmed by 1.9 Å resolution crystal structure, Tyr_Z is hydrogen bonded to D1-His190 (2.5 Å distance) (Fig. 8A) [18]. It is assigned as a proton acceptor to Tyr_Z by several methods (site-directed mutagenesis, FTIR and structural modeling) [36, 39-45]. Additionally, Tyr_Z is connected either directly to W4 or through the additional water molecules to W3, W2 and W1. D1-His190 is connected through the series of amino acids and water molecules to the luminal bulk solution. The amino acid residues lying along the way of this channel to the lumen belong to the D1, Cp43 and PsbV subunits. The charged amino acid residues (D1-Arg323, D1-His304 and PsbV-Lys129) surround the exit of this channel [18].

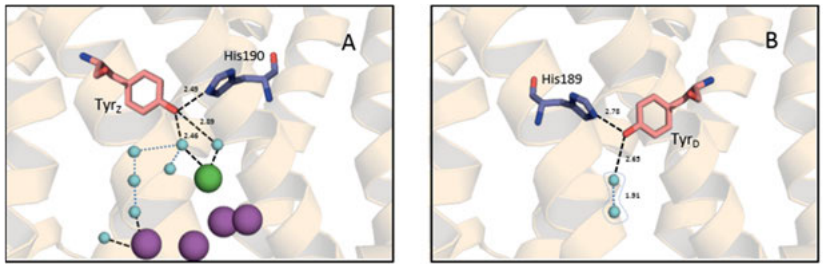

Figure 8. The environment around Tyr_Z (A) and Tyr_D (B).

Contrary to Tyr_Z, Tyr_D (Tyr-160) is deeply buried in the hydrophobic environment of the D2 protein. It is positioned symmetrically to Tyr_Z in the D2 protein. The homologous to D1-His190, D2-His189 was identified in the vicinity of Tyr_D (Fig. 8B). A single water molecule was found in the hydrogen bond distance to Tyr_D. It is not completely occupied in the structure, but there are indications for the two possible positions of this water molecule in the vicinity of Tyr_D [18, 46]. The hydrogen bonding patterns of both tyrosines determined their functional differences and mechanistic aspects of oxidation which will be discussed in the section below.

Functional differences

Tyr_Z bears a highly oxidizing potential (E_m $Tyr_Z^{\bullet}/Tyr_Z$ > 900–1000 mV) which makes oxidation of water at the Mn_4CaO_5 cluster possible [47]. Under illumination, Tyr_Z acts as a relay between highly oxidative P_{680}^{+} and Mn_4CaO_5 cluster. It is a two steps process: i) oxidation of Tyr_Z by P_{680}^{+} in the nanosecond to microseconds time scale, ii) the reduction of $Tyr_Z^{\bullet}$ by the Mn_4CaO_5 cluster in the microseconds to millisecond time regime [45, 48-51].

Tyr_Z is a neutral radical in the oxidized state. Upon Tyr_Z oxidation, phenolic proton is transferred to the nearby D1-His190 residue. This proton is transfered back after Tyr_Z reduction. The process does not require significant rearrangement in the system, which is why the Tyr_Z oxidation can occur in a fast nsec/μsec timescale. However, the oxidation of Tyr_Z is S-state dependent, multiphasic and a very fast process. It is 20-40 ns in the S_0 and S_1 states while, at higher S-states, it slows to 50 ns in S_2 and 260 ns in S_3 states respectively [48, 52, 53]. In 20 % of PSII centers, Tyr_Z

undergoes oxidation in a microsecond time scale [49, 53, 54]. For a long time it was thought that the slow microsecond kinetics reflects inactive PSII centers. But later it was assigned to the centers with less defined hydrogen bonding environment around Tyr_Z, which restricts very fast deprotonation reaction. Tyr_Z oxidation is pH independent between pH 5.5 and 8.0. The rate and amplitude of Tyr_Z oxidation decreases towards acidic pH with pK_a 4.5-5.3, which was attributed to the titration of D1-His190, causing disordering of the essential hydrogen bonding [55, 56].

Its symmetrical counterpart in the D2 subunit, Tyr_D, does not undergo such fast oxidation behavior [57]. It is not involved in the water oxidation, but still was conserved throughout evolution. The role of Tyr_D in PSII has been the subject of continual research [38, 58-61]. Tyr_D is oxidized by S_2 or S_3 state with a half-time tens of sec at pH range between 5 and 7.5, forming a long-lived tyrosine radical ($Tyr_D^{\bullet}$) [47, 62]. It slowly decays over hours in the dark. Tyr_D has a slightly less positive oxidation potential E_m = 700-800 mV if compared to Tyr_Z [36, 63]. Both tyrosines are positioned the same distance to P_{680} (12.4 Å away), and can be oxidized by P_{680}^+ [18]. However, due to the slow oxidation at physiological pH Tyr_D is not competitive to Tyr_Z as an electron donor to P_{680}^+. Tyr_D oxidation rates becomes efficient, comparable to those seen for Tyr_Z, at elevated pH with a pK_a~7.6 ($t_{1/2} \approx$ 190 ns) [38]. Like Tyr_Z, Tyr_D is involved in PCET reaction, getting protonated or deprotonated upon reduction or oxidation respectively. Earlier publications suggested that D2-His189 is the proton donor to the reduced state of Tyr_D as the symmetrical counterpart D1-His190 to Tyr_Z [45, 64-67]. However, the recent crystal structure at 1.9 Å identified also a water molecule in the hydrogen bonded distance from Tyr_D, which can occupy proximal or distal positions [18, 46]. As has been reported independently by spectroscopic studies and calculations, the proximal water molecule accepts phenolic proton upon oxidation of Tyr_D [46]. The mechanism of Tyr_D oxidation will be discussed in detail in papers I and II.

It can be concluded that the key to the functional difference of Tyr_Z and Tyr_D is determined by the fate of the proton upon tyrosine oxidation. The oxidation of Tyr_Z in nsec timescale is due to the proton-rocking mechanism of the hydrogen bond between D1-His190 and Tyr_Z, while the slow oxidation of Tyr_D is due to the movement of water molecule, serving as a proton acceptor with subsequent release of proton to the bulk. The crucial role of Tyr_Z in PSII has been demonstrated in many studies. However, the role of Tyr_D PSII is still unclear. There are several

postulated roles of Tyr_D in PSII: i) it acts as an electron acceptor from Mn_4CaO_5 cluster in the lowest state of S-cycle (S_0), it stabilizes the cluster to the higher and more stable state in the dark (S_1); ii) it has a role in the oxidation of over-reduced forms of Mn during photoassembly of WOC [64, 68, 69]; iii) it has an electrostatic effect to the localization of cation in the P_{680} moiety [57, 70, 71]. Regardless of the proposed possible roles of Tyr_D in PSII, the undeniable fact is that Tyr_D is conserved in all photosynthetic species, and the growing Tyr_D-less mutants have some difficulties [57].

Interaction of tyrosines with S-states of WOC

$Tyr_Z^{\bullet}$ is able to oxidize all S-states of WOC. The fast oxidation and reduction of $Tyr_Z^{\bullet}$ in the presence of WOC makes it difficult to study. One of the important probes in this respect are the metalloradical EPR signals [72]. When two paramagnetic species are located at a short distance (5-10 Å) from each other, their spins magnetically interact, forming very distinct set of EPR signals. The nature of such interaction is due to a spin exchange interaction or between the magnetic dipoles of the electrons [73]. The interaction of the Tyr_Z and Mn_4CaO_5 cluster is one of them. The prerequisite for this interaction is the formation of Tyr_Z radical under continuous illumination at cryogenic temperatures at which WOC is not able to turn over, as this will cause the appearance of so called EPR split signals. Except for the transient S_4 state, interaction of all S-states with $Tyr_Z^{\bullet}$ gives rise to the Split signals (Fig. 9) [74, 75]. Interaction of Tyr_Z with the S_1 state of Mn_4CaO_5 cluster was a subject of study in Paper VI.

Contrary to Tyr_Z, $Tyr_D^{\bullet}$ can only oxidize S_0 state of WOC. It is very slow process taking from minutes to hours at room temperature [35]. The oxidation of Tyr_D occurs by only the S_2 and S_3 states. It is pH dependent reaction accelerating towards higher pH [47]. The oxidation of Tyr_D by the S_2 or S_3 states is biphasic process with fast and slow phases governed by water position in the vicinity of Tyr_D. The population of PSII centers with water in the proximal position give rise to the fast, pH independent oxidation phase and the population of PSII centers with water in the distal position induce the slow, pH-dependent oxidation phase. The biphasic kinetics was observed at pH<7.3 and one phase for pH>7.3 [47].

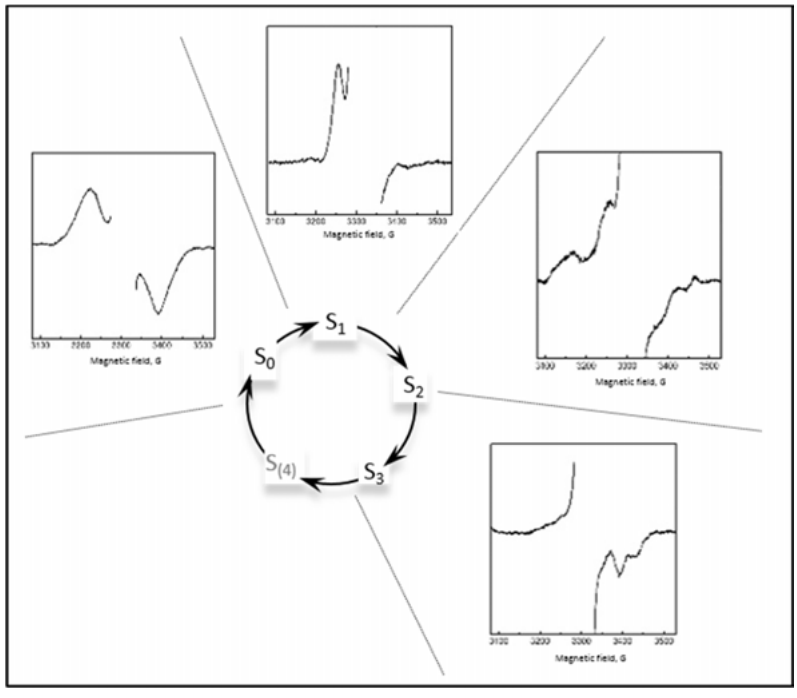

Figure 9. Summary of the Split EPR signals from different S-states induced in PSII by illumination at low temperature. The middle part of each spectrum from overmodulation $Tyr_D^{\bullet}$ is removed for clarity.

Methods

Electron Paramagnetic Resonance

Electron paramagnetic resonance is a technique for the detection of unpaired electrons in a molecular system. The method has been notably used in the detection of transition metals, radicals, triplets, etc., and, therefore, is extremely informative in studying the electron transfer reaction. The system with unpaired electrons is called paramagnetic, and without unpaired electrons, diamagnetic. An electron has a magnetic moment induced by the two properties: spin and charge. In the presence of a magnetic field, the magnetic moment can be oriented parallel or antiparallel to the magnetic field. Each orientation requires specific energy due to the Zeeman effect:

$$E = m_s g_e \mu_B B_0$$

g_e – known as the electron´s g-factor, or Lande´s factor, g_e= 2.0023 for free electron; μ_B is the Bohr magneton. If microwave energy matches with the energy difference of these two states, an unpaired electron absorbs energy *hv* and changes spin. The absorption leads to the rise of an EPR signal.

Commoner observed an EPR signal from PSII first time in 1956, which later was known as a Signal II_{slow} or Signal II_D [76]. It was a stable radical signal with g=2.0046 and decay halftime in min-hours time range [58]. Later it was identified that signal comes from tyrosine radical and was called Tyr_D (index D derived from the word *"dark"* due to its stability in the dark). Tyr_D signal is considered to be a robust signature for PSII quantification. Afterwards, by improved EPR spectrometer, similar to Signal II_{slow}, signal with fast decay kinetics was observed in Mn-depleted PSII [77]. The signal has msec-sec decay halftime and was called Signal II_{fast}. Further studies assigned Signal II_{fast} to the Tyr_Z radical of PSII.

Soon, the third type of Signal II, Signal $II_{very\ fast}$, was detected in intact PSII samples, with a very fast decay halftime (μsec-msec) [78].

In 1981, EPR signal from Mn_4CaO_5 cluster was reported in thylakoid membranes [79]. It showed a period of four oscillations with every applied laser flash. The signal appeared after the first and fifth flash. It was concluded that this is a signal from S_2 state of the cluster, the so-called S_2 multiline signal (Fig.10). Later, signals from other S-states of Mn_4CaO_5 cluster were also discovered, except for the transient S_4-state (Fig.10).

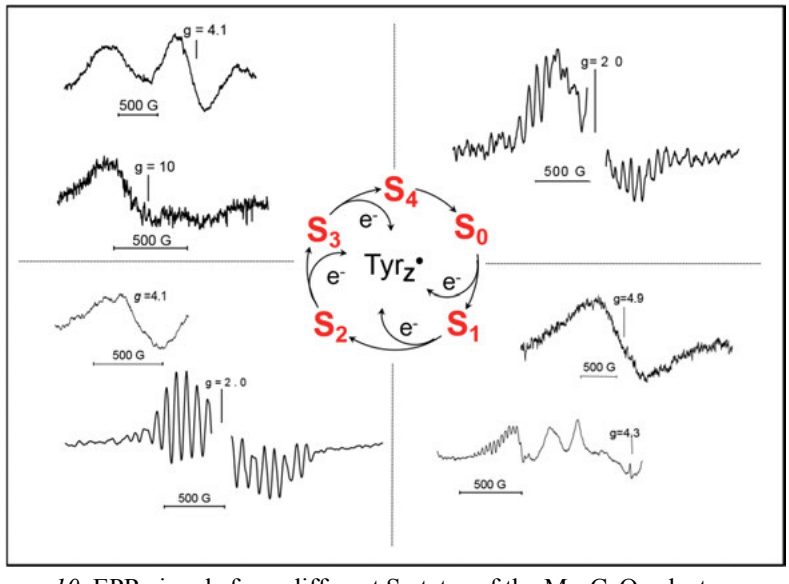

Figure 10. EPR signals from different S-states of the Mn_4CaO_5-cluster.

Another cofactor of the electron transport chain detected by EPR spectroscopy is Cyt b_{559}. Cyt b_{559} exhibit rhombic signals with anisotropic g values (g_z approx. 3.0, g_y approx. 2.2, and g_x approx. 1.5), varying in different preparations. The anisotropic g values represent the orientation of the heme relative to the membrane plane which, in turn, affect the redox potential of Cyt b_{559}. The heme was found to be perpendicular to the membrane plane in the oxidized and reduced states of Cyt b_{559}. Slight variations in the *g*-values of the redox form of Cyt b_{559} reflects changes in the heme environment of the different form [29].

The high spin signal originated from $Q_A^-Fe^{2+}$ interaction has a characteristic EPR signal with *g* value around 1,82 [80]. $Q_A^-Fe^{2+}Q_B^-$ interaction signal is detected with *g*=1,66 [81].

Photoxidizible Chl and carotenoids molecules can also be detected by EPR spectroscopy. Photoinduced P_{680}^+ has *g*=2,0027 with line width 10 G. The spin-polarized triplet signal from $^3P_{680}$ with the zero-field splitting parameters $|D| = 0.0286\ cm^{-1}$, $|E| = 0.0044\ cm^{-1}$ is another detectable EPR signal from PSII. It is formed due to $Pheo^-P_{680}^+$ recombination [82].

Fluorescence

The light energy absorbed by Chls molecule can undergo one of the three possible pathways: i) it can be used to drive photochemistry (water splitting reaction); ii) it can be dissipated as heat; or iii) be re-emitted as light (so called chlorophyll fluorescence) [83]. These pathways are competing, the increase of one will lead to the decrease of the another two pathways. Re-emission of excess energy as heat or fluorescence is a protective mechanism of the system against high light conditions. Hence, measurements of the yield of chlorophyll fluorescence has been used to obtain information about the integrity and changes in the photosynthetic electron transport chain [84, 85]. In 1931, Kautsky and coworkers observed for the first time an increase in the yield of chlorophyll fluorescence for approximately 1 sec after exposing dark adapted leaves to light [86]. The rise was later assigned to the reduction of acceptors in PSII, namely Q_A. In the dark adapted the "open" PSII centers exhibit very low fluorescence yield, Q_A is able to accept one electron, and, after illumination, an electron is on Q_A during this period, and the reaction center is called "closed," and is highly fluorescent [87, 88]. After an electron passes further in the chain to Q_B, the decay of fluorescence is observed [89, 90]. The flash-induced variable fluorescence is one of the fluorescence techniques to follow this decay. After a saturating flash, the rise of fluorescence is observed from F_0 level when all reaction centers are open, and low fluorescent to F_{max} when all Q_A is reduced and reaction centers are closed and highly fluorescent. The following dark adaptation leads to the subsequent decay of fluorescence. The difference in changed fluorescence yield is called variable fluorescence. The observed decay of fluorescence reflects the reoxidation of Q_A^- [89, 91]. The kinetics consists of three exponential phases with lifetimes in microseconds, milliseconds and seconds time

scale, and can vary depending on PSII material. The fast phase is assigned to electron transport from Q_A^- to Q_B or Q_B^- , which is bound to the Q_B-site. The middle phase in msec time scale is attributed to those centers which did not have Q_B bound before the flash, and requires time for new Q_B to bind. The third slow phase originates from centers where Q_B is not available and Q_A^- recombines with the S_2 state of Mn_4CaO_5-cluster. When the forward electron transfer is blocked by the herbicide addition, for example DCMU, an electron stays on Q_A for a few seconds and slowly decays via the $Q_A^-S_2$ recombination [90, 92].

Thermoluminescence

Thermoluminescence is a weak light emission from irradiated materials with trapped charge separated states upon being heated. The light emission comes from a recombination of photoinduced charge pairs when the thermal energy of the environment matches with the activation energy barrier of two separated charges. Thermoluminescence is widely used as a dating technique in archeology. Thermoluminescence from photosynthetic systems were first observed by Arnold and Sherwood in 1957 [93]. They observed light emission peak at 30-40 ^oC from dried chloroplast samples, illuminated prior to the heating, which they explained as the release of stored energy upon heating. Later, it was assigned to the recombination of different cofactors in PSII [94, 95].

Table 1. *The temperature peak and origin of TL bands*

TL component	Peak temperature ^oC	Charge pair
B_1-band	~ +30 to +40	$S_2Q_B^-$
B_2-band	~ +30	$S_3Q_B^-$
Q-band	~ +5	$S_2Q_A^-$
A-band	~ -15	$S_3Q_A^-$
C-band	~ +50	$Tyr_D^+Q_A^-$

The rate of recombination can be brought down to a negligible level if samples are cooled down immediately after illumination; then heating up progressivly reveals the appearance of different thermoluminescence bands. Photoinduced charge pairs are stabilized by the activation energy barriers (ΔG) limiting back flow. Thermoluminescence from PSII originates mostly by the recombination of the following charge pairs: $S_2Q_B^-$,

$S_3Q_B^-$, $S_2Q_A^-$. Thermoluminescence bands detected in PSII samples are summarized in Table 1 [94].

The protonation state around $Tyr_D/Tyr_D^{\bullet}$ and redox equilibrium in Photosystem II

The proton coupled electron transfer reaction is a fundamental property of the energy conversion in biological systems [96]. In many enzymes, processes like catalysis and charge transport are often underpined due to the coupling of a proton transfer to an electron. Such coupling helps biological systems to stay neutral, avoid high energy pathways, and the formation of unfavorable species in the oxidation-reduction processes. One example of PCET reactions is the oxidation and reduction of the two tyrosines (Tyr_Z and Tyr_D) in PSII [97]. These tyrosines represent an ideal model system to study PCET reaction of two identical species in a different protolytic environment.

In Paper I, the mechanism of PCET of Tyr_D was studied by using CW EPR and deuterium isotope effect on the Tyr_D oxidation behavior under different pH conditions. In Paper II, in addition to the Tyr_D oxidation kinetics at different pH, the competing recombination reactions, which involved the acceptor side of PSII, were investigated by using the variable flash-induced fluorescence and thermoluminescence techniques.

Tyr_D oxidation kinetics consists of two phases: fast and slow. A fast phase is essentially pH-independent both in amplitude and lifetime, while a slow phase exhibits a strong pH-dependence [47]. The biphasic behavior of the oxidation kinetics of Tyr_D was previously assigned to two distinct proton equilibria associated with the oxidation of Tyr_D by the S_2 state. One of these proton equilibria was suggested to be in the vicinity of Tyr_D, and the other near the Mn_4CaO_5 cluster [47]. According to this model, biphasic kinetics are observed when the Tyr_D oxidation process is faster than the proton equilibria near Tyr_D and the Mn_4CaO_5 cluster. The deprotonated and protonated populations in this case are independent from each other. Contribution of each population to the fast and slow phases respectively, have a pH-independent lifetime. However, the amplitude of each phase would be pH-dependent due to the changes in the

relative degree of protonation. It changes the relative size of protonated and deprotonated Tyr_D populations. Contrary, if the proton equilibrium is faster than Tyr_D oxidation, it causes the reestablishment of the equilibrium prior to oxidation of Tyr_D and a monophasic kinetic behavior is observed. We further advanced the results obtained in [47] with incorporation of some important differences.

The Tyr_D oxidation kinetics were followed in a deuterated buffer over a wide pD range (4.7-8.7). The time resolved kinetics in a deuterated buffer at pD 6.3 differed significantly both in amplitude and in half-time compared to non-deuterated. The kinetics were observed to be slower by more than a 3–fold for the fast phase and almost by a 10-fold for the slow phase. The full kinetic analysis of amplitudes and half-times is summarized in Fig.11

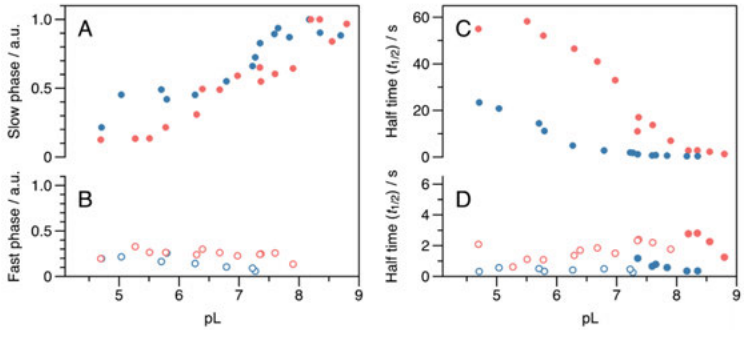

Figure 11. Amplitudes and half-times of the two kinetic phases in the oxidation of Tyr_D in pH (blue) or pD (red) buffers. A and B show the amplitudes of the slow (filled circles) and fast (open circles) kinetic phases as a function of pL. C and D show the half-times of the two phases as a function of pL.

The kinetics were fitted by two exponential phases, for pH < 7.3 and pD < 8.0, and one phase for pH > 7.3 and pD > 8.0. Hence, at lower pL the oxidation of Tyr_D was biphasic (fast and slow phases), whereas at high pL only monophasic oxidation behaviour was observed. The amplitude of the slow phase was strongly pL-dependent and decreased towards lower pL values from about 90% to 20-30% (Fig. 11A). Contrary to the slow component, the fast component was independent at pL below 7.5 (Fig. 11B). The half-times of the fast phase were almost pH independent, moderate pD-dependence was observed (Fig. 11D). The half-time of slow phase was again pL dependent. It decreased towards higher pH/pD value and eventually merged with the half-times of the fast phase by

forming monophasic Tyr_D oxidation kinetics (Fig. 11C). The half-time of the slow phase ranged from 23 sec at pH 4.7 to <1 sec at pH 8.7 in non-deuterated buffers, while in deuterated buffers it changed from 50 sec at pD 4.7 to 1-2 sec at pD 8.7.

The rate constants for the slow phase were calculated as a function of pL (k_H for non-deuterated and k_D for deuterated buffers) (Fig. 12). The KIE for whole pL range was calculated by taking into account the degree of protonation/deuteration. This was accomplished using the pK values from the data in Fig. 12. For the detailed explanation of the fitting parameters, see Paper I.

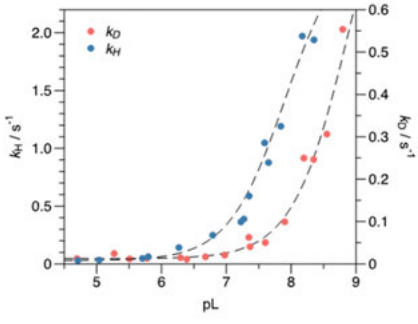

Figure 12. pL dependence of the rate constants for $Tyr_D^{\bullet}$ formation in the slow phase in pH (blue) with pK 7.9 and pD (red) buffers with pK 8.9.

The recent crystal structures of PSII revealed a water molecule in the vicinity of the phenol group of Tyr_D which can occupy two positions [18]. The proximal position of the water molecule is 2.6-3.2 Å away from the phenolic oxygen of Tyr_D and the distal position is 4.3-4.5 Å. In Paper I, we proposed that the equilibrium between these two possible water molecule positions gives rise to two distinct populations of PSII centers. At low pH, the fast phase in the Tyr_D oxidation corresponds to those centers where a water molecule occupies the proximal position, and hydrogen bonded to the phenolic proton of Tyr_D which is released during its oxidation (Fig. 13). According to the DFT-QM/MM calculations [46], this water molecule accepts a proton released upon Tyr_D oxidation and moves to the distal position. Then proton accepted by the water molecule transferred further to the D2-Arg190 and is released via proton channel out to the lumen. This proton release to the lumen after Tyr_D oxidation has been recently shown by FTIR experiments [98]. However, at higher pH values, the phenolic proton of Tyr_D is already titrated away, and only electron transfer process takes place. This is the reason for the pH-independency of the fast component of Tyr_D oxidation kinetics (Fig. 13). In contrast, the slow pH-dependent kinetic phase is assigned to the centers with the water molecule already in the distal position. In this case, the water position is the rate-limited step for the Tyr_D

oxidation process. Tyr_D does not have a direct hydrogen bond to the water molecule, and deprotonation of Tyr_D can only happen after the distal water comes close enough to accept the proton through thermal motion without being in the fully occupied proximal position (Fig. 13). Since water is not readily available to accept the released proton, it makes the oxidation of Tyr_D slower. Towards higher pH values, the amount of the deprotonated Tyr_D populations are increasing, which makes convergence of the slow component with the fast component of Tyr_D oxidation kinetics. It leads to the higher amplitude and eventually only monophasic Tyr_D oxidation kinetics, with pK 7.9 in H_2O and 8.9 in D_2O. Therefore, the overall rate of Tyr_D oxidation increases with pH as well.

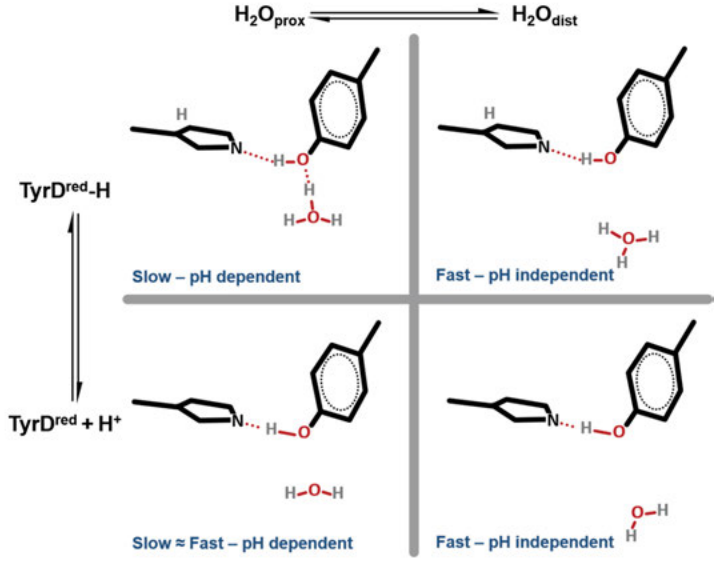

Figure 13. The changes of the hydrogen bond prior the Tyr_D oxidation depending on protonation state (up/down) and water position (left/right) affecting the kinetics of Tyr_D oxidation.

Equations 2-6 in Paper I shows the model of Tyr_D oxidation with the fast proton equilibrium where k_{prot} and k_{dep} are the oxidation rate constants of protonated and deprotonated Tyr_D, respectively.

The calculated kinetic isotope effect (KIE) was around 2.3-2.5. The origin of KIE was attributed to the proton/deuterium, which is in the strong hydrogen bond between Tyr_D and D2-His189.

In Paper II, we observed that limitations of the acceptor side of PSII strongly affected the kinetics of Tyr_D oxidation. The addition of DCMU, which binds in the Q_B-site of PSII and blocks the forward electron transfer from Q_A, led to the complete elimination of the slow phase of the Tyr_D oxidation kinetics (Fig. 14). Consequently, the total yield of the oxidized Tyr_D was also altered, and only 18% at pH 4.7, 24% at pH 6.3 and 72% at pH 8.5 was observed (Fig. 14). The difference in the amplitude of oxidized Tyr_D with or without DCMU was 33% at pH 4.7, 39% at 6.3, and only 6 % at pH 8.5. This difference corresponds exactly to the population of PSII contributing to the slow phase of Tyr_D oxidation.

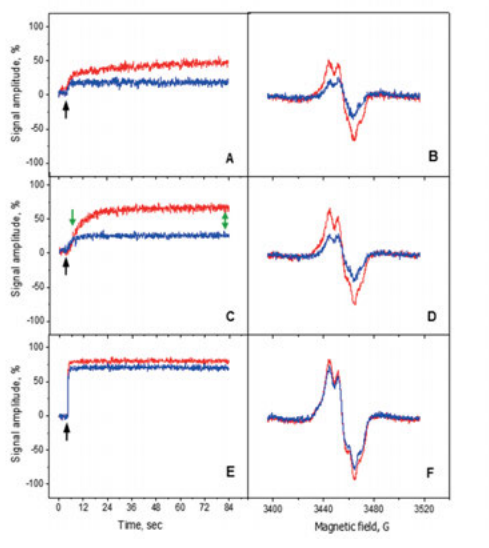

Figure 14. Oxidation of Tyr_D after a single flash at different pH values at RT. Kinetic traces (left: A, C, E) and field-swept (right: B, D, F) in the absence (red line) or presence of 1.75 mM DCMU (blue line) at pH 4.7 (A and B), pH 6.3 (C and D) and pH 8.5 (E and F).

To follow the possible contribution of other cofactors in PSII to Tyr_D oxidation, samples were frozen about 3 sec after the laser flash (indicated by the green arrow in Fig. 14, and EPR measurements were performed at low temperature. In the samples without DCMU addition, within 3 sec after the flash, 100 % of the S_2 state multiline EPR signal was detected at pH 6.3 (Fig. 15). However the presence of DCMU lowered the S_2 state multiline signal to 82 % (Fig. 15). The decrease in the multiline signal was assigned to $S_2Q_A^-$ state recombination which occurred before the freezing. Complete decay of the signal was observed after 80 sec in the presence or absence of DCMU. The similar pattern was observed at pH 4.7. Only 90 % of the S_2 state multiline was detected within 3 sec after the flash in the absence of DCMU. As was reported before, the decrease in the amplitude is due to the pH-dependence of the S_2 state multiline signal. In the presence of DCMU, 70 % of the S_2 multiline signal was observed at 3 sec after the flash. At pH 8.5 no S_2 multiline signal was detected.

The oxidation of Tyr_D occurs via the WOC, namely by the reduction of the S_2 state to the S_1 state via equilibrium with P_{680}^+ and $Tyr_Z^{\bullet}$.

$$S_1\ Tyr_D \xrightarrow{light} S_2\ Tyr_D \xrightarrow{dark} S_1\ Tyr_D^{\bullet}$$

This was first suggested in [47], but was never experimentally proven. Our results showed indeed verify the rise in the amplitude of Tyr_D oxidation accompanied by the decay of the S_2 state multiline signal (Fig. 15).

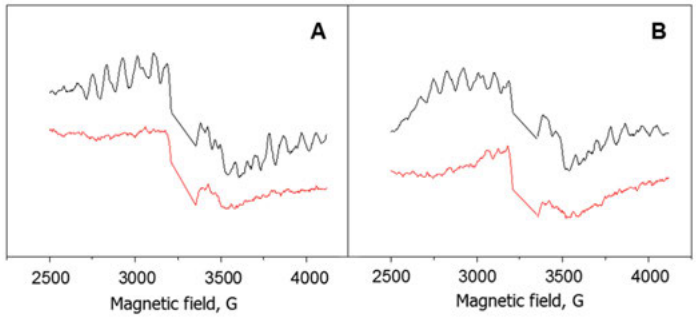

Figure 15. The S_2 state multiline EPR signal in samples with reduced Tyr_D frozen 3 sec (black spectrum) or 80 sec (red spectrum) of laser flash at pH 6.3 in the absence (A) or presence of 1.75 mM DCMU (B).

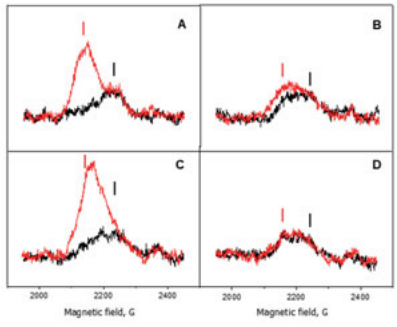

Figure 16. EPR spectra of the g_z region of oxidized Cyt b_{559} in samples with reduced Tyr_D at pH 6.3 in the absence (A, B) or presence of 1.75 mM DCMU (C, D). Spectra in A and C were recorded from samples before laser flash (black spectra) or after 6 min illumination at 77 K (red spectrum). Spectra in B and D were recorded after 3 sec (black spectrum) or 80 sec (red spectrum) of laser flash.

Another redox component in PSII is Cyt b_{559} (Fig. 16). The flash induced oxidation of the high potential form of Cyt b_{559} at pH 4.7 and 6.3 was observed (Fig. 16, g=3.05). We observed 10 % at pH 6.3 and 16 % at pH 4.7 oxidation of the Cyt b_{559} 3 sec after the flash. An additional 10 % at pH 6.3 and 6 % at pH 4.7 oxidation of the Cyt b_{559} was detected 80

sec after the flash. No oxidation of Cyt b_{559} was observed in the presence of DCMU. Interestingly, there were no changes in the redox state of Cyt b_{559} at pH 8.5.

To follow the competing acceptor side recombination with Tyr_D oxidation for the S_2 state recombination, the flash-induced fluorescence decay kinetics were measured. Fig.17 shows the flash induced fluorescence kinetics at three pH values in samples with Tyr_D in the oxidized (black traces) and reduced form (red traces). No difference was observed in the kinetics of fluorescence decay between Tyr_D oxidized and Tyr_D reduced samples at pH 4.7 and 6.3. Contrary, at pH 8.5, samples with Tyr_D in reduced form demonstrated a non-decaying slow phase of the fluorescence kinetics. This non-decaying phase was assigned to the centers where Tyr_D oxidation outcompetes the $S_2Q_A^-$ recombination reaction. The non-decaying phase was more pronounced in the presence of DCMU (Fig. 17). We observed the difference between samples with Tyr_D^{ox} and Tyr_D^{red} at all three pH when the forward electron transfer from Q_A^- was inhibited, and re-oxidation of Q_A^- is only possible via S_2 state recombination. The difference in amplitude of the slow phase between Tyr_D ox-

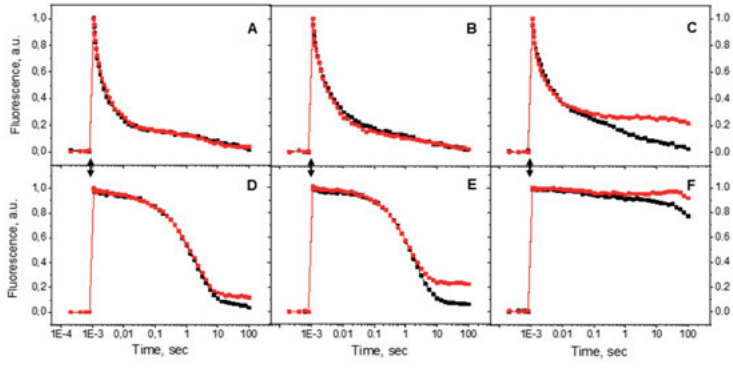

Figure 17. Flash-induced variable fluorescence decay traces from samples with Tyr_D reduced (red traces) and oxidized (black traces) in the absence (A, B, C) or presence of 20 μM DCMU (D, E, F) at pH 4.7 (A, D), pH 6.3 (B, E) and pH 8.5 (C, F).

idized and reduced samples was increasing at higher pH (Table 2 in Paper II). Interestingly, the difference can reach 40 % of the total variable fluorescence at pH higher than 8.0 (Paper II, Suppl. Fig. 2).

Our fluorescence measurements indicated that the redox state of Tyr_D does not have any effect on the forward electron transfer in PSII. However, the inhibition of the forward electron transfer (with DCMU addition) gave rise to the appearance of a difference between PSII samples with oxidized and reduced Tyr_D. The difference correlated well with the amplitude of the fast phase of Tyr_D oxidation kinetics. Therefore, it can be concluded that the population of Tyr_D which undergoes the fast oxidation clearly wins the competition with the $S_2Q_A^-$ state recombination. We observed an even more pronounced effect at pH 8.5 where the fast phase of Tyr_D oxidation was dominant.

The recombination reaction, in addition to fluorescence measurements, was studied by thermoluminescence (Fig. 18) The B1-band which reflects $S_2Q_B^-$ recombination was found at 39 ^oC at all three pH values in the Tyr_D oxidized PSII samples. However, in the Tyr_D reduced PSII samples, the peak of the B1 band was shifted down to 31 ^oC and amplitude was 4 times lower at pH 4.7, and 2.5 times lower at pH 6.3. The amplitude of the B1 band in Tyr_D oxidized samples was significantly decreased at pH 8.5 compared to the lower pH, and completely absent in the Tyr_D reduced samples. The observed difference in the amplitude and temperature peak between samples with Tyr_D in oxidized and reduced state reflects the changes in the free energy gap, ΔG between the two charge separated component Q_B^- and the S_2 state. The lower free energy gap ΔG between the charge separated state at lower temperature the recombination will take place. The shift of the peak detected in Tyr_D reduced samples could be caused by an absence of the positive charge on Tyr_D. In addition, the loss in the amplitude of the Tyr_D reduced samples can also be assigned to the competing Tyr_D oxidation reaction. The presence of DCMU induces the Q-band peak around 10 ^oC, which is attributed to the $S_2Q_A^-$ recombination. In the Tyr_D oxidized PSII samples, the Q-band glowed at 9 ^oC at pH 4.7 and 6.3. PSII samples with Tyr_D in reduced state showed the upshift of temperature peak to 13 ^oC at pH 4.7 and 6.3. The Q-band of Tyr_D oxidized samples at pH 8.5 was shifted to 34 ^oC, with significant lower amplitude than at pH 4.7 or 6.3, and was almost absent in Tyr_D reduced samples.

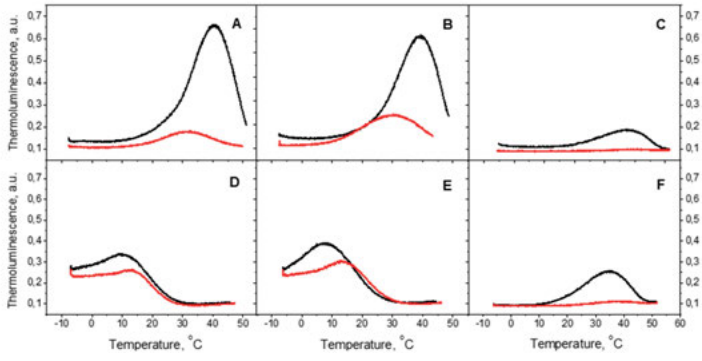

Figure 18. Thermoluminescence bands obtained in samples with Tyr_D in reduced (red traces) and oxidized (black traces) in the absence (A, B, C) and presence of 40μM DCMU (D, E, F) at pH 4.7 (A, D), pH 6.3 (B, C) and 8.5 (C, F).

The kinetics model for Tyr_D oxidation and competing electron transfer steps is summarized in Fig. 19. There are six possible acceptor/donor side reaction pathways that lead to $Tyr_D^{\bullet}$ formation: in two steps after electron transfer to Q_B (k1/k3; k1/k4; k2/k3; k2/k4), or in one step with the acceptor-side electron still on Q_A (k3/k4). The results of this kinetic modeling are summarized in Fig. 7 Paper II, which correspond well with the experimental data. Our experimental data, kinetic modeling of the Tyr_D oxidation and competing recombination reaction in Paper II confirmed the existence of two distinct populations of PSII centers with respect to the redox state of Tyr_D: the slow oxidized population which is in the competition due to similar halftime with recombination reactions, and the fast oxidized population of Tyr_D which is always prevalent over recombination reactions.

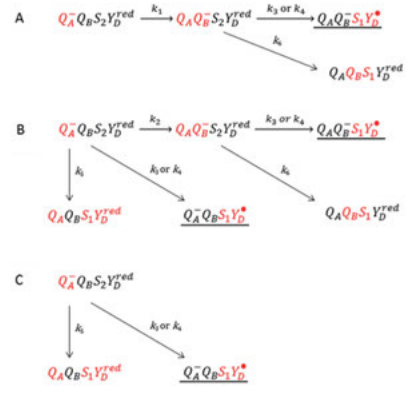

Figure 19. Kinetics models for electron transfer after initial transition of PSII to the S_2 state.

Far-red light triggered induction of P_{680}^{+} and tyrosine radicals formation

PSII photochemistry is a complex process affected by several factors, of which the light quality is the most important. Absorption of light by Chl promotes an electron from the ground state (S_0) to the singlet excited state (S*i*). The greater the energy in the absorbed photon, the higher the excited singlet state transition will be initiated. The type of chlorophyll molecules and their arrangement defines the energy required for this transition. There are at least five different chlorophyll found in oxygenic photosynthetic organisms: Chl *a, b, c, d, f*. These chlorophylls are presented with differences in their absorption wavelength. This difference is not only tuned by the protein environment but also by the distinct chemical composition of each of the chlorophyll molecules respectively. [24]. Nearly all chlorophylls in the photosynthetic organisms are associated with specialized proteins: antenna proteins or reaction center proteins.

The reaction center of PSII, P_{680}, consists of four Chl molecules bound by the D1/D2 heterodimer denoted as P_{D1}, P_{D2}, Chl_{D1} and Chl_{D2}, (Fig. 24). P_{D1} and P_{D2} are weakly excitonically coupled to the central Chl pair, and are situated at a 30° angle to the horizontal plane. The other two Chls, Chl_{D1} and Chl_{D2}, are located symmetrically on either side of P_{D1} and P_{D2} respectively (Fig. 23). The excitation energy transfer to the reaction center Chls of PSII initiates the primary charge separation. The formation of the first stable Chl cation after the primary charge separation reaction, has been monitored extensively by various spectroscopic methods [99-104]. There are indications that the first Chl electron donor is different when PSII is excited by the far-red light (720-800 nm) if compared to visible light (400-700 nm).

To investigate the localization of the primary Chl donor under far-red light, the spin polarized triplet state of $^3P_{680}$ and the difference in the oxidation efficiency of Tyr_Z and Tyr_D were used as probes in Paper III and IV respectively.

The prerequisite for the formation of the spin polarized triplet $^3P_{680}$ state is the double reduction of Q_A. The double reduction of Q_A was achieved by a prolonged incubation of PSII samples in the presence of a reducing agent, sodium dithionite and a mediator, benzyl viologen. Under these conditions, the double reduced Q_A becomes protonated and presumably released from its binding site. As a consequence, the long-lived charge-separated state $P_{680}^+ Pheo_1^-$ decays via slow recombination to allow spin dephasing to the spin-polarized triplet state.

The illumination of the reduced samples with visible light at cryogenic temperatures (5 K), induces the formation of a characteristic EPR signal arising from the spin polarized $^3P_{680}$ with high yield (Fig. 20). We have attempted the induction of the triplet signal under far-red light illumination (>730 nm) however, no spin polarized $^3P_{680}$ EPR signal was detected under these conditions, even after meticulous accumulation (Fig. 20). Several reasons have been postulated to explain the above observation: I) The far-red light is not efficient to drive photochemistry. However, this can be ruled out because the efficient far-red photochemistry of PS II has been demonstrated before. In addiiton we have observed the accumulation $Pheo^-$ signal under these conditions [99]. II) The formed $^3P_{680}$ signal decays faster than can be detected. This possibility was tested by the decay kinetic measurements of the $^3P_{680}$ signal induced at different wavelengths (Paper III, Fig. 6). No differences were observed in the decay kinetics under different wavelength. III) We propose that the primary electron donor to Pheo is different under far-red light illumination compared to visible light. Most studies suggest that the primary cation formed under visible light is P_{D1}. This well explains the triplet formation under visible

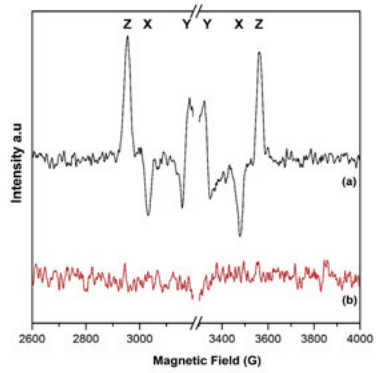

Figure 20. Light-dark difference EPR spectra of the spin-polarized $^3P_{680}$ in PS II samples with (a) white light and (b) far-red light (732nm) at 5 K

light, since the recombination between $Pheo^-$ and P_{D1} is slow enough to allow spin dephasing. In contrast, we suggest that under far-red light illumination, reduction of Pheo occurs from Chl_{D1}. It has been previously experimentaly observed that, the Chl_{D1}^+ is close enough to oxidize Tyr_Z, but too far for the oxidation Cyt b_{559}/Chl_Z/Car pathway [100]. The close proximity of Chl_{D1} to Pheo allows for fast recombination without spin dephasing, which essentially prevents the formation of the spin polarized $^3P_{680}$ (Fig. 20).

To test this hypothesis at room temperature, the oxidation of two tyrosines in Mn-depleted samples were followed by EPR spectroscopy under visible and far-red light conditions, at different pH values (Fig. 21). The reduction of Tyr_D was achieved by prolonged dark incubation at

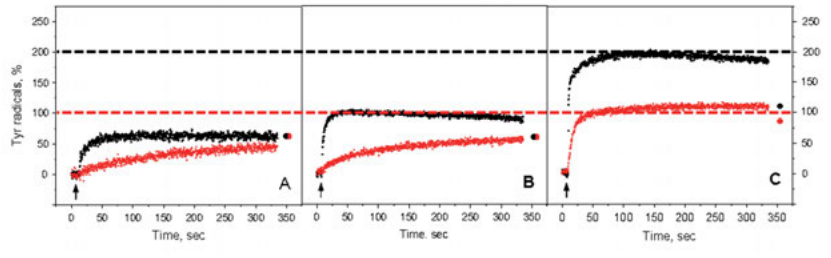

Figure 21. Kinetics of tyrosines oxidation recorded at 3465 G under continuous white light (black traces) or far-red illumination (red traces) at pH 4.7 (A), pH 6.3 (B), pH 8.5 (C) in Mn-depleted PSII samples.

room temperature. Steady state oxidation of Tyr_Z and Tyr_D under continuous illumination with white or far-red light resulted in a different yield of Tyr oxidation depending on pH. The yield of Tyr oxidation increased upon increase of pH, with the maximum at pH 8.5. The yield of Tyr oxidation was lower at all measured pH under the far-red light illumination, compared to white light illumination. The decreased yield of $Tyr^\bullet$ under far-red light illumination could be due to either i) less effective charge separation; or ii) the different primary electron donor which drives a less efficient far-red photochemistry. The first hypothesis can be ruled out because the accumulation of $Pheo^-$ indicates that most of the PSII centers undergo charge separation [99]. Oxidation of both tyrosines were observed under white light illumination at pH 8.5, while the far-red light induced only $Tyr_D^\bullet$ formation. The difference between these two wavelengths can be attributed to either a different tyrosine oxidation pathway (Tyr_D and Tyr_Z) or the different nature of the primary donor.

To distinguish between the $Tyr_Z^{\bullet}$ and $Tyr_D^{\bullet}$ signal formation at all three pHs, a sequence of flash-induced measurements in the absence and presence of an effective electron donor to Tyr_Z (DPC) and acceptor from Q_B-site (ferricyanide) was performed (Paper IV Fig. 5, 6, 7). Tyr_Z oxidation was observed at all three pH values and under both 532 and 732 nm flashes (Paper IV Fig. 3). The amplitude of $Tyr_Z^{\bullet}$ was both pH and wavelength dependent. However, the calculated decay half-time values of $Tyr_Z^{\bullet}$ have shown significant pH dependence (Paper IV, Table 1).

There are three possible donors to $Tyr_Z^{\bullet}$: Tyr_D, DPC (if present), or recombination with the acceptor side (Fig. 22). In the presence of DPC, the amplitude of the $Tyr_Z^{\bullet}$ radical formation was significantly inhibited, especially under 732 nm flashes at pH 4.7 and 6.3 (to 3 and 25 % respectively). This resulted in significantly less formation of $Tyr_D^{\bullet}$ especially with the 732 nm flashes. Based on the above, it can be concluded that, at pH 4.7 and 6.3, oxidation of Tyr_D occurs via the $Tyr_Z^{\bullet}$ radical according to the following reaction:

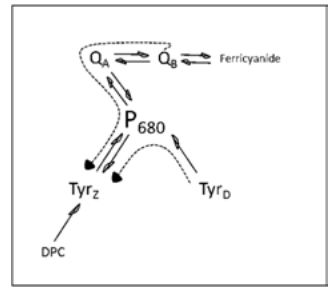

Figure 22. Electron transfer events upon Tyr_Z and Tyr_D oxidation reaction

$$Tyr_D Tyr_Z \xrightarrow{light} Tyr_D Tyr_Z^{\bullet} \longrightarrow Tyr_D^{\bullet} Tyr_Z$$

Contrary to the low pH, at pH 8.5 and in the precense of DPC, a significant amount of $Tyr_D^{\bullet}$ was still formed. The absence of the fast decay on the first flash (Paper IV Fig. 7) at pH 8.5 indicates the direct Tyr_D donation to P_{680}^{+} under both light conditions.

Our results also confirm that the far-red light induced photochemistry occurs in the majority of PSII centers. Interestingly, the far-red light results in decreased $Tyr_Z^{\bullet}$ formation at normal and low pH values at room temperature. We attribute the latter observation to the higher recombination rate from the acceptor side under far-red light illumination. We propose that increase in the recombination rate is due to the different cation localization in P_{680}^{+} (Fig. 23).

Both the formation of the spin polarized $^3P_{680}$, as well as the oxidation of the two tyrosines in PSII, indicate the existence of a difference in the primary photochemisty between these two wavelengths. The proposed

different cation localization is based on the following structural differences between the Chl of P_{680} ensemble: The special Chl pair of P_{680}, P_{D1} and P_{D2} has a weak electronic coupling due to the greater physical separation, a slight difference in the tetrapyrrole ring orientation and a smaller dipole strength of the Q_y transition [105-107]. The latter results in a pair that does not represent the lowest energy sink for the excitation energy. Since the monomeric Chl_{D1} does not have such coupling, it is believed to be the lowest energy sink for the excitation energy [107]. Therefore, the migration of the far-red exciton among the four Chl molecules in P_{680} would not be an energetically favorable process. Thus, we conclude that, under far-red light excitation, the primary hole is localized on Chl_{D1}.

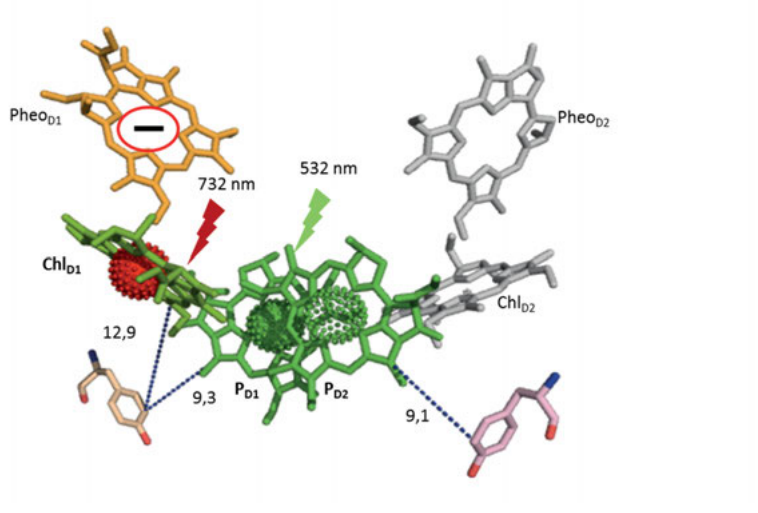

Figure 23. Primary charge separation in PSII under far-red (732 nm) and visible light (532 nm)

Role of the PsbTn subunit in steering H^+ from Tyr_D

The recent single particle CEM structure revealed four extrinsic protein subunits, namely PsbO, PsbP, PsbQ and PsbTn , on the luminal side of the eukaryotic PSII complex [1]. The PsbO, PsbP, and PsbQ subunits form the triangular crown shape structure interacting with the luminal domain of the C-terminal of the D1 protein and CP43. These shield the WOC from any exogenous reductant on the luminal side. The PsbO, PsbP, PsbQ subunits can be easily removed by "washing" the PSII preparations with various reagents and their loss leads to the deactivation of WOC, with subsequent release of a Mn_4CaO_5 cluster from a site. Meanwhile, as a tightly bound protein PsbTn remains bound after the washing procedures [108-110]. The role of the PsbTn subunit has been unknown [111, 112]. In Paper V, we investigated the role of the PsbTn subunit in the redox reactions of Tyr_D.

In our experiments we used PSII membrane preparations from Arabidopsis thaliana WT and three deletion mutants, ΔPsbTn1, ΔPsbTn2

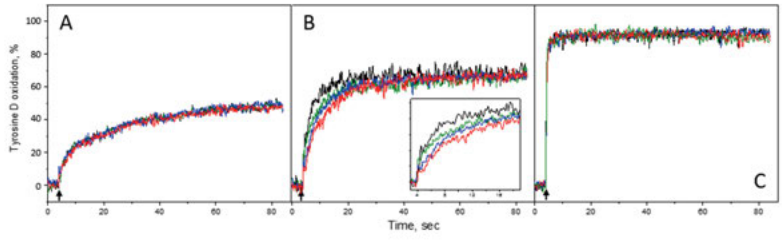

Figure 24. Tyr_D oxidation kinetics at 3445 G at pH 4.7 (A), 6.3 (B) and 8.5 (C) measured in PSII membranes with the reduced Tyr_D from the WT (black traces), ΔPsbTn1 (green traces), ΔPsbTn2 (blue traces) and ΔPsbTn1+2 double mutant (red traces). Arrows indicate the time position of the laser flash.

and ΔPsbTn1+2. Tyr_D was chemically reduced prior to measurements according to [47, 113]. The Tyr_D oxidation kinetics were followed at three pH values by using time-resolved EPR spectroscopy (Fig. 24). The Tyr_D oxidation kinetics of the WT sample were observed as biphasic at pH 4.7 and 6.3, accelerating at higher pH values, leading to monophasic oxidation kinetics being observed at pH 8.5 (Fig. 24). These observations corresponds to the oxidation behavior of Tyr_D reported earlier [113-115]. The Tyr_D oxidation kinetics in ΔPsbTn1, ΔPsbTn2 and ΔPsbTn1+2 followed the same kinetics as Tyr_D in WT samples at pH 4.7 and 8.5 (Fig. 24A, C). Interestingly, at pH 6.3 the kinetics of Tyr_D oxidation were different from the WT in all three mutants (Fig. 24B). The kinetics slowed down from ΔPsbTn1 to ΔPsbTn2 and ΔPsbTn1+2, respectively. Changes in the amplitude and half-time of both phases were observed (Table 2).

Table 2. The total yield of $Tyr_D^{\bullet}$ and the amplitude of the fast and slow phases ($t_{½}$, sec and amplitude (%)) were obtained after two exponential growth fitting of traces shown *in Fig. 24.*

	Wild Type	ΔPsbTn1	ΔPsbTn2	ΔPsbTn1+2
$Tyr_D^{\bullet}$	100%	71%	89%	89%
Fast phase	1.64 (51%)	3.77 (45%)	4.80 (35%)	5.48 (27%)
Slow phase	8.89 (49%)	18.80 (55%)	21.29 (65%)	52.20 (73%)

It is known that the Tyr_D radical slowly decays in the dark by reduction from S_0 state of the Mn_4CaO_5 cluster and other components. The decay

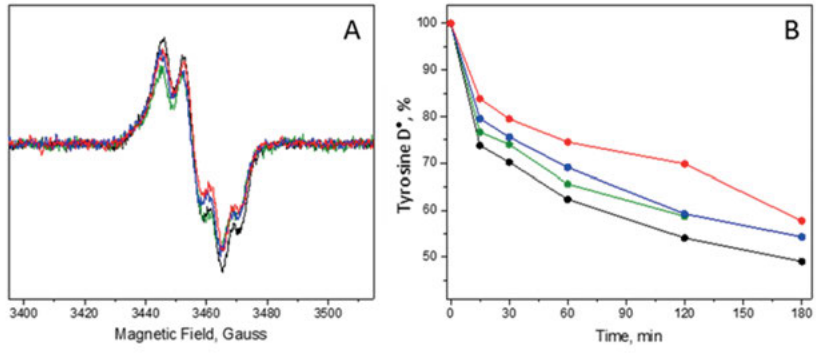

Figure 25. The total yield of $Tyr_D^{\bullet}$ induced by continuous illumination at pH 6.3 (A) and with subsequent decay during the dark adaptation (B) in PSII membranes from the WT (black), ΔPsbTn1 (green), ΔPsbTn2 (blue) and ΔPsbTn1+2 double mutant (red)

of Tyr_D radical was monitored during a three hour period at pH 6.3 in WT and PsbTn mutants (Fig. 25). The decay of $Tyr_D^{\bullet}$ was also different in the mutants. The double PsbTn1+2 showed the slowest decay among all mutants if compared to the WT (25% after 2 hours vs 45%).

In Paper I and II, we assigned fast and slow phases of Tyr_D oxidation kinetics to the two populations of PSII centers with water molecules at the proximal or distal positions. When water occupies the proximal position, it is in a slow equilibrium with the lumen, and the Tyr_D oxidation is fast (Fig. 13). The occupancy of water in the distal position results in a fast proton equilibrium with the lumen, and slow oxidation of Tyr_D is observed (Fig. 13). Only the slow phase is affected by pH. The removal of PsbTn results in the slow oxidation kinetics of Tyr_D and deceleration of the decay of the Tyr_D radical. PsbTn is found on the luminal side of the D2 protein forming a bridge between PsbE and CP47. The distance of Tyr_D from the PsbTn subunit is about 16 Å, and situated directly under it (Fig. 26A). We propose that the PsbTn subunit is shielding the H^+-

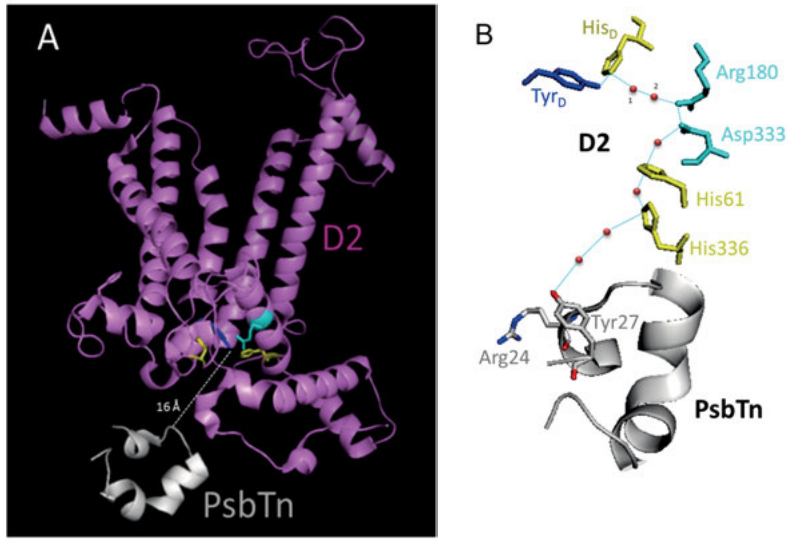

Figure 26. PsbTn and D2 proteins interaction, side view (A) (PDB code 3JCU) and molecular interactions and putative H^+-channel leading from Tyr_D to the PsbTn protein (B) (PDB code 3JCU, [1]). Water molecules (red dots) are included manually.

channel exit from $Tyr_{D,}$ and subsequent removal of it leads to the alteration of the existing equilibria of the distal and proximal water with the lumen (Fig. 26B). Additionally, the possible buffering role of PsbTn subunits on Tyr_D oxidation is not excluded.

The Donor-Acceptor side interactions in Photosystem II

PSII has two quinones, Q_A and Q_B on the acceptor side of PSII, symmetrically located on either side of the non-heme Fe^{2+}. Despite their identical chemical structure (PQ-9), they differ in functionality and redox potential. Q_A is an immobile cofactor well buried inside the D2 protein that functions as one electron carrier, accepting electrons from $Pheo^-$ and reducing the second quinone acceptor, Q_B. Q_B is one of the quinones of the plastoquinone pool which is bound to the Q_B-pocket. Q_B acts as a two electron and two proton carrier. After the double reduction and protonation steps, Q_BH_2 leaves the Q_B-site in the plastoquinole form to be replaced by a new PQ-9 from the plastoquinone pool. All these events presumably require some conformational rearrangement in the vicinity of the protein.

There are several lines of evidence for a long-range interaction between the donor and acceptor sides in PSII: i) alteration of the redox potential of Q_A upon perturbation at the donor side [116-120]; ii) the removal of bicarbonate causes the loss of the S_2 state EPR multiline signal [114]; iii) the effect of herbicide binding at the Q_B-site on the redox potential of Q_A [121, 122] and the position of Cl^- ion in the vicinity of the Mn_4CaO_5-cluster [123]. The mechanism of such a long interaction remains unclear.

To experimentally approach the long range transmembrane conformational rearrangement between the acceptor and donor side in PSII, in Paper V, we studied how the total yield of Tyr_Z oxidation at cryogenic temperature depends on biding the native or exogenous quinones at the Q_B-site. The S_1 split signal was used as a probe, to estimate the relative amount of PSII centers with Tyr_Z in the oxidized form.

The Q_B-site is located close to the protein surface, which makes it quite sensitive to detergent treatments. Different solubilization steps during the PSII membrane preparation results in the different state of the Q_B-site. In our study, to estimate the Q_B-site occupancy by the native PQ-9 (Q_B) in different PSII preparations, the flash-induced fluorescence kinetics were measured. Preparations 1 and 2 (with the mild detergent treatment) showed the fast decay phase of fluorescence kinetics with a half-time of 700 μsec and an amplitude of 45 %, indicating fast electron transfer from Q_A^- to bound Q_B (Fig. 27). In preparations 3 and 4 (with the

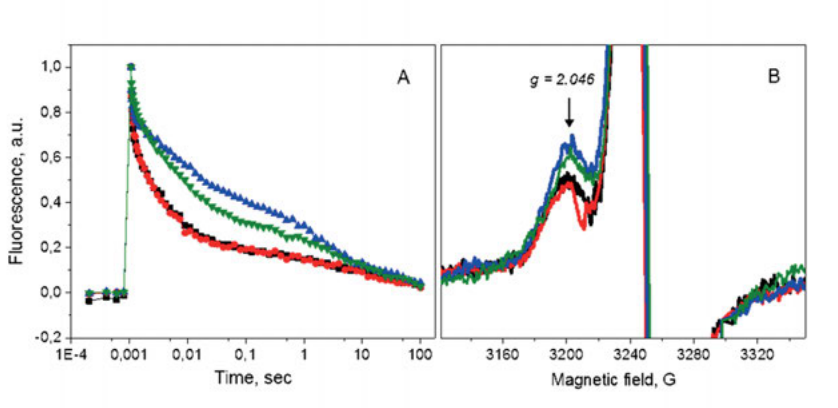

Figure 27. A – Flash-induced fluorescence decay kinetics from different PSII preparations with different occupancy of the Q_B-site. B -The S1 split EPR signal induced in the corresponding preparation at 5 K illumination. Preparation 1 and 2 (black and red traces and spectra) are two PSII preparations obtained with gentle detergent treatment and preparation 3 and 4 (green and blue traces and spectra)

harsh detergent treatment), the fast phase is only comprised of 25 % (Fig. 27). The preparations with higher fast phase amplitude (1 and 2) were thus identified as PSII centers with high occupancy of the Q_B-site (~45 %), while preparations with the lower fast phase amplitude were assigned to the centers with low occupancy of the Q_B-site (~25 %, Table 1, Paper VI). The S_1 split EPR signal was induced in these preparation by illumination at 5 K. Interestingly, preparations 1 and 2 with the high Q_B-site occupancy gave rise to the lower S_1 split signal amplitude (by about 20-25%), if compared to preparations 3 and 4 with low occupancy of the Q_B-site (Fig. 27).

The native quinone PQ-9 (Q_B) can be oxidized or replaced by a number of plastoquinone analogs. These have been widely used to estimate the rates of oxygen evolution. They vary in structure, E_m and the ability to accept electrons from PSII. Oxygen evolution measurements were performed in the presence of different electron acceptors dissolved in DMSO. The highest rate of O_2 evolution was observed in the presence of DCBQ and PpBQ, 383 and 257 μmol of O_2 mg $Chl^{-1}h^{-1}$ respectively. Lower oxygen evolution rates were observed in samples with DMBQ and ferricyanide, 125 μmol of O_2 mg $Chl^{-1}h^{-1}$ and DQ with 100 μmol of O_2 mg $Chl^{-1}h^{-1}$. Samples with either the native quinones PQ-9 present in the preparation, or exogenous quinones PQ-10, HQ and DBMIB did not produce any oxygen evolution.

The S_1 split EPR signal measured in the presence of the exogenous quinones showed different amplitudes. In order to draw a correlation between the S_1 split signal formation and the state of Q_B-site, the oxidation of Cyt b_{559} and $Q_A^-Fe^{2+}Q_B^-$ signals were also measured by EPR spectroscopy. The presence of only DMSO, which was the solvent used in all additions in this study induced 6-fold increase of the S_1 split signal if compared to samples without any additions. The addition of PpBQ, DCBQ, DMBQ, DQ and HQ led to a further increase of the S_1 split signal (Paper VI Table 3, Fig. 2). Interestingly, the highest amplitude was observed in the presence of quinones which are not efficient electron acceptors in PSII (PQ-10, HQ and DMBQ). They also resulted in the high amplitude of the $Q_A^-Fe^{2+}Q_B^-$ (Paper VI Table 3; Fig.2). It was clear that although different quinones had different effect on the Q_B-site, their presence influenced the formation of the S_1 split EPR signal on the donor side of PSII.

The presence of DMSO, a small molecule that has access to the H-bonding network of the Q_B-pocket had similar effect [124]. In the crystal structure of PSII, two molecules of water at the Q_B-site were found, hydrogen bonded to D1-Tyr246 and the oxygen atom of the bicarbonate. It was suggested that the position of water changes upon herbicide binding, thus inducing a stabilizing effect. We proposed that DMSO disturbs or replaces these water molecules, which leads to the conformational changes. The binding of the exogenous quinones into the Q_B-pocket likely further enhances these changes.

The amplitude of the S_1 split signal can be affected by the following: (i) changes in the magnetic coupling between the Mn_4CaO_5 cluster and

$Tyr_Z^{\bullet}$, or (ii) if the number of PSII centers with well-defined low barrier Tyr_Z-His_Z hydrogen bond and with less-defined bond is changed.

Based on the results reported in this study, we propose the following mechanism for the long-range interplay between the state of the Q_B-site and the redox state of Tyr_Z. One of the amino acids involved in the hydrogen bonding of Q_B, His_B is located on the same transmembrane α-helix of the D1 protein, helix D, as His_Z, the proton acceptor of Tyr_Z at the distance of about 36 Å at the opposite side of the membrane (Fig. 28). This lower part of helix D has a different membrane orientation and also known as the CD helix (Fig. 28). We suggest that changes which occur at the Q_B-site in the His_B protonation state when Q_B is not bound lead to the helix D tilting towards the C2 axis of the PSII, altering the H-bonding distance between His_Z and Tyr_Z. Most probably, this bond becomes more optimal for H to be translocated upon oxidation of Tyr_Z. The latter occurs at room temperature. In the frozen samples, this configuration is preserved, and subsequent illumination of samples at cryogenic temperature leads to the formation of the different amount of $Tyr_Z^{\bullet}$.

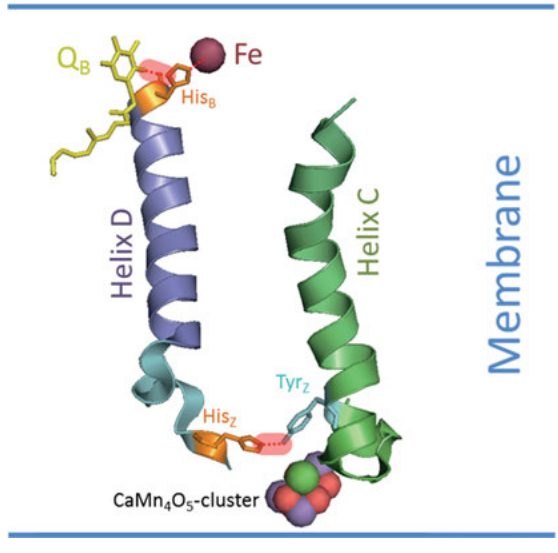

Figure 28. Arrangement of Q_B and His_B and Tyr_Z and His_Z on the helix D of the D1 protein of PSII within the thylakoid membrane. Hydrogen bonds are indicated by red dotted lines and highlighted.

Sammanfattning

Den globala energikonsumtionen fortsätter att öka i takt med en mer utbredd industrialisering och en ökad befolkningsmängd. I dag är den årliga förbrukningen i världen totalt 16,3 terawatt (TW), av vilken EU och USA använder 40 %. Energianvändningen beräknas öka till ca.20 TW år 2030 och mer än fördubblas jämfört med detta fram till år 2050. I nuläget är 85 % av energin producerad från fossila råvaror. De återstående 15 % kommer från kärnkraft, vattenkraft och olika förnybara energikällor som exempelvis biomassa, vindkraft och solceller. Den stora användningen av fossila bränslen leder oundvikligen till stora utsläpp av koldioxid (CO_2), som är en strakt bidragande orsak till den globala uppvärmningen. Som ett svar på detta måste vi nu utveckla nya tekniker för energiomvandling som istället bygger på en förnyelsebar och miljömässigt ren energikälla. Ett exempel på en sådan energikälla är strålningen som kommer från solen. Varje år träffas jorden av solstrålar med en energi motsvarande ca.100 000 TW, alltså långt mer än vårt nuvarande energibehov.

Naturen har löst uppgiften att använda solenergi på ett effektivt sätt i en process som kallas fotosyntes. Genom fotosyntesen produceras årligen biomassa motsvarande 100 miljarder ton. Nyckeln bakom denna effektiva produktion av biomassa från solenergi är den i princip obegränsade tillgången till råmaterial. Allt som behövs är energi från solen, koldioxid och vatten. Fotosyntesen är naturens kraftverk som genererar energirika molekyler, med syrgas som en bi-produkt. Den första formen av fotosyntes fanns hos föregångarna till dagens cyanobakterier redan för mer än 3 miljarder år sedan. Nu finns fotosyntesen hos både bakterier och eukaryoter (alger och växter). Fotosyntesen (den syrgasproducerande varianten) kan beskrivas genom följande förenklade reaktion:

$$6CO_2 + 6H_2O \xrightarrow{h\nu} 6(CH_2O) + 6O_2$$

där 6(CH_2O) representerar de energirika molekylerna (kolhydrater). Syrgasproducerande fotosyntes kan delas upp två skilda processer, en ljusbereoende och en ljusoberoende. Den ljusberoende processen sker i speciella membran (thylakoid-membran) inuti cellerna. I dessa membran hittar men fyra stora proteinkomplex, enzymer, som är kopplade till fotosyntesen; fotosystem II (PSII), cytokrom b_6f, fotosystem I (PSI) och ATP syntas (se bild 2). Energi skapas genom att protoner flyttas från en sida av membranet till den andra samtidigt som elektroner passerar genom de olika proteinkomplexen. Den koncentrationsskillnaden som uppstår över membranet används av ATP syntas för att bilda energirika ATP molekyler. Den ljusoberoende processen använder sedan de energirika molekyler som produceras (ATP tillsammans med NADH) för att, i flera steg i den så kallade Calvin-Benson-Bassham cykeln, bilda kolhydrater från koldioxid (CO_2). Om den sinnrika omvandlingen av energi i fotosyntesen kunde kopieras på konstgjord väg skulle vi kunna skapa en förnyelsebar och ren energiförsörjning. En artificiell fotosyntes skulle kunna producera energirika bränslen såsom vätgas eller metan och samtidigt minska koldioxidutsläppen i atmosfären. Ju mer vi kan lära oss av den naturliga fotosyntesen ju större är möjligheten att skapa en artificiell fotosyntes som bygger på naturens principer.

Målet med denna avhandling är att bidra med kunskap kring processerna i fotosyntesen med speciellt fokus på funktionen av det unika enzymet PSII, som oxiderar vatten med hjälp av ljus. I artikel I och II i denna avhandling har en redox-aktiv co-faktor, aminosyran tyrosin D (Tyr_D), studerats i detalj. I artikel I undersöktes hur deuterium påverkar oxidationen av Tyr_D med hjälp av elektron paramagnetisk resonans (EPR) spektroskopi. I artikel II analyserades sedan hur oxidationen påverkas av kompeterande reaktioner i enzymet med hjälp av ljusblixt-inducerad fluorescens och termoluminiscens. Det har visat sig att oxidationen av Tyr_D kan observeras med två olika hastigheter, en snabb och en långsam. I artikel I och II diskuteras orsaken till dessa två faser, och hur de påverkas av proton (pH) och deuterium koncentration. Till stöd användes information från de senaste detaljstrukturerna av PSII, bestämda genom röntgenkristallografi och teoretiska beräkningar (DFT-QM/MM). Från resultaten kunde vi föreslå hypotesen att de två faserna härrör från två olika strukturer av PSII, som skiljer sig åt genom positionen av en vattenmolekyl i närheten av Tyr_D. Vid låga pH observerades den snabba fasen från PSII där vattenmolekylen binder Tyr_D via en vätebindning, och därmed underlättar oxidationen av Tyr_D (se bild 13). Vid oxidationen

flyttar vattenmolekylen längre ifrån Tyr_D och liknar då också den struktur som ger upphov till en långsammare oxidering av Tyr_D. Oxidationen av Tyr_D kan endast ske när vattenmolekylen befinner sig tillräckligt nära Tyr_D för att ta emot en proton från Tyr_D, eller vid högt pH när protonen i vätebindningen inte längre finns där.

I artikel III och IV har vi studerat de processer som är inblandade när energin från ljuset fångas upp av PSII. Ljuset absorberas av speciella klorofyllmolekyler som slutligen ger en laddningsseparation i proteinet. Hur effektiv absorptionen är beror bland annat på ljusets våglängd, energiinnehåll. För att studera hur ljusets våglängd påverkar laddningsseparationen har vi studerat triplet-tillståndet hos klorofyll (^{3}Chl) i PSII, tillsammans med oxidationen av Tyr_D och Tyr_Z som är en följd av laddningsseparationen. Det visade sig att när ljus av längre våglängd (732 nm) användes för excitation så kunde elektronhålet primärt lokaliseras till en klorofyllmolekyl, Chl_{D1}, medan ljus av kortare våglängder (532 nm) gav ett mer delokaliserat elektronhål spritt över flera klorofyllmolekyler i PSII (se bild 23).

Flera redox-aktiva co-faktorer driver tillsammans oxidationen av vatten i PSII och ser samtidigt till att minimera risken för skadliga bi-reaktioner. I artikel V studerade vi på vilket sett co-faktorn Tyr_Z är involverad i långskaliga reaktioner i PSII (interaktioner mellan donator- och acceptorsidan i proteinet). Genom att använda blixt-inducerad fluorescens i kombination med EPR spektroskopi var det möjligt att följa interaktionen mellan Tyr_Z och acceptorn quinon B (Q_B). Från detta var det möjligt att dra följande slutsatser; i) oxidationen av Tyr_Z påverkas av redoxtillståndet hos Q_B och ii) utbytet av Q_B mot en annan quinon leder till förändringar i proteinstrukturen som i sinn tur påverkar vätebindningen mellan Tyr_Z och dess granne His_Z.

PSII består av mer än 30 olika subenheter (proteiner). I växter och alger finns det fyra specifika proteiner exponerade på ytan (PsbO, PsbP, PsbQ och PsbTn). Tre av dessa, PsbO, PsbP, PsbQ, sitter nära det aktiva center där vatten oxideras till syre och elektroner, och är nödvändiga för ett funktionellt PSII komplex. Rollen för den fjärde subenheten, PsbTn, är däremot fortfarande okänd. I artikel VI undersökte vi hur PsbTn påverkar redox-aktiviteten hos Tyr_D med hjälp av en mutant som saknar PsbTn. Resultaten från mätningar med EPR spektroskopi visade att saknaden av PsbTn förändrar oxidationshastigheten och stabiliteten hos Tyr_D. Detta visar på en möjlig roll för PsbTn i protontransporten i närheten av Tyr_D.

Xülasə

Global enerjisinin istehlak sürəti sənayenin və dünya əhalisinin sayının fasiləsiz artımı səbəbi ilə daim yüksəlir. Hal-hazırda istehlakın norması 16.3TW təşkil edir, bunun 40%-i AB və ABŞ payına düşür. Güman olunur ki, bu rəqəm 2030-cu ildə 20 TW və daha çox, 2050-ci ildə isə iki dəfədən də çox artmış olacaq. Hal-hazırda global istehlak enerjisinin təqribi 85% -i qalıq yanacaq hesabına əmələ gəlir. Qalan 15%- i isə nüvə, hidroelektrik,biokütlə, külək və günəş panelləri və s. kimi bərpa olunan enerji mənbələridir. Qalıq yanacağın yanması geniş CO_2 emissiyasina səbəb olur. CO_2 istixana effekti qazlarından biri olub, atmosferdəki istiliyi tutaraq qlobal istiləşməyə səbəb olur. Bu problemi həll etmək üçün, biz enerjinin - bolluğu, bərpaolunan olması, təhlükəsiz və təmiz olması prinsiplərinə əsaslanan yeni texnologiyaları inkişaf etdirməyə çalışırıq. Bəşəriyyət üçün mövcüd olan belə mənbəllərdən biri günəş enerjisidir. Planetimizə düşən illik günəş enerjisinin miqdarı təqribi 100 000 TVt təşkil edir, hansı ki, bu ehtiyacımızın daha artıqdır. Təbiət günəş enerjisinin mənimsənilməsi məsələsini fotosintez prosesi nəticəsində həll edir. Fotosintez nəticəsində əmələ gələn biokütlə 100 milliard ton quru çəki kimi qiymətləndirilir, hansı ki, təqribi 100 TVt enerjiyə uyğun gəlir. Bu təbii fenomenin, fotosintezin, uğurunun böyük miqyaslı olması prosesin getməsi üçün xammalın yəni, günəş enerjisi, su və karbon qazının sonsuz miqdarı ilə əlaqədardır.

Fotosintez təbiətin günəş enerjisindən zəngin enerjiyə malik molekul və oksigen qazı emal edən fabrikidir. Mövcüd geokimyəvi dəlillərə əsasən, bu prosesin yaranması 3 milliard il bundan əvvələ təsadüf edir. Oksigenli fotosintezi həyata keçirən ilk orqanizm müasir sianobakterianın əcdadı olmuşdur. Hal-hazırda, fotosintez həyatın iki fundamental sahəsi, bakteriya və eukariotlar (bitki və yosun) tərəfindən həyata keçirilir. Oksigenli fotosintez aşağıdakı reaksiyaya qədər sadələşə bilər:

$$6CO_2 + 6H_2O \xrightarrow{h\nu} 6(CH_2O) + 6O_2$$

$6(CH_2O)$ enerji ilə bol məhsulu (karbohidrat) xarakterizə edir. Oksigenli fotosintez iki tip reaksiyalar toplusundan ibarətdir : işıqdan asılı olan və işıqdan asılı olmayan reaksiyalar. Oksigenli fotosintetik orqanizmlərdə, işıqdan asılı reaksiyalar xüsusi tilakoid membranlarda həyata keçirilir. Bu 4 böyük zülal superkomplekslərində həyata keçirilir Fotosistem II (FSII), Sitoxrom b_6f (Cyt b_6f), Fotosistem I (FSI) və ATF sintaza (ATF) (Sxem 2). Elektronlar elekton zəncirindən keçdiyindən enerjiləri, protonları stromadan lümenə ötürülməsi nəticəsində proton qradientinin əmələ gəlməsinə sərf olunur. Transmembran proton qradienti ATF-i əmələ gətirən ATF sintaza adlı kompleks zülalı hərəkət etdirir.

Işıqdan asılı və qaranlıqda baş verən reaksiyalar xloroplastların stromasında baş verir. Bu reaksiyalar iki molekul, hüceyrənin energetik valyutası adlanan, işıq fazasında sistez olunan NADFH və ATF hesabına baş verir. Qaranlıq fazanın reaksiyaları CO_2 –dən karbohidrat sintez etmək üçün bir neçə fermentativ addımlardan , ümumilikdə Calvin-Benson-Bassham adlanan tsikldən ibarətdir.

Əgər biz fotosintezə bənzər effektiv süni sistemlər yaratmaqda uğur qazansaydıq, bu insanlığın enerji ilə bağlı tələbatını ödəməyə kömək edərdir. Süni fotosintez hidrogen, metan kimi yüksək enerjiyə malik yanacaqla təmin etməklə yanaşı, eyni zamanda atmosferdə CO_2 miqdarını olduqca azalda bilərdi. Biz təbii fotosintezin mexanizmini daha dərindən öyrəndikcə, biomimetrik davamlı süni sistemləri yaratmaqda uğur əldə edə bilərik.

İşin əsas məqsədi, təbii fotosintez barədə biliklərimizi dərinləşdirmək, əsasən də onun unikal fermentinin fəaliyyətini, FSII, öyrənməkdən ibarətdir. FSII də olan bir redoks aktiv Tyr_D-kofaktorların oksidləşmə mexanizmi öyrənilmişdir (Məqalə I və II). Deyterium izotopunun effekti Tyr_D- oksidləşməsində EPR ilə öyrənilmiş və Məqalə I mövzusu olmuşdur. Məqalə II Tyr_D oksidləşməsinin kinetikasına əlavə olaraq, FSII akseptor hissəsini cəlb edən, rəqabətli rekombinasiya reaksiyaları, işıqla-induksiyaolunmuş flüoressensiya ilə yanaşı, termolüminessensiya metodları ilə də öyrənilmişdir. Tyr_D oksidləşməsi iki fazadan ibarətdir: sürətli və yavaş faza. Hər iki məqalədə Tyr_D oksidləşməsinin sürətli və yavaş komponentlərin mexanizmi, onların pH (-dan) asılılığı və kinetik izotop məlumatlar yüksək ayırdetmə qabiliyyətinə malik FSII kristallik quruluşu haqqında və Tyr_D oksidləşməsinin DFT-QM/M ilə yaxın

zamanlardakı tədqiqatlar nəticəsində alınan məlumatlar əsasında müzakirə olunmuşdu.

Məqalə I və Məqalə II alınmış nəticələrə əsasən, təklif olundu ki, bu iki su molekulunun yerləşməsi arasındakı tarazlıq, FS II –nin iki populyasiyası hesabına baş verir.

pH-in aşağı səviyyəsində Tyr_D oksidləşməsinin sürətli fazası elə mərkəzlərə uyğun gəlir ki burada, su molekulu daha yaxın məsafədə yerləşir və Tyr_D fenolik protonu ilə əlaqəli hidrogen, hansı ki, onun oksidləşməsi nəticəsində azad olmuşdur (şək. 13). Bu su molekulu Tyr_D oksidləşməsi zamanı buraxılan protonu qəbul edir və periferik vəziyyətə doğru hərəkət edir. Lakin, pH-in yuxarı qiymətlərində, Tyr_D fenolik protonu artıq uzaqda titrlənir və yalnız elektonların ötürülməsi prosesi baş verir. Bu Tyr_D oksidləşmə kinetikasının sürətli komponentinin ph-dan asılı olmadığının səbəbidir. Əksinə, ph-dan asılı yavaş faza periferik vəziyyətdə yerləşmiş su molekulunun mərkəzinə təyin olunur. Bu zaman Tyr_D oksidləşməsi prosesi üçün suyun vəziyyəti məhdud dərəcədədir. Tyr_D deprotonlaşması yalnız o halda mümkün ola bilər ki, periferik su kifayət qədər yaxınlaşaraq istilik hərəkətindən protonu tuta bilsin, eyni zamanda tamamilə proksimal vəziyyətdə olmasın. Suyun buraxılmış protonu asanlıqla tuta bilməməsi Tyr_D oksidləşməsini gecikdirir.

FSII fotokimyası kompleks proses olub, bir sıra faktorlardan asılı ola bilir. Onlardan biri işıqdır. Işığın xlorofillərin reaksiya mərkəzi FSII tərəfindən udulması, bu kompleks prosesdə ilkin yüklərin ayrılmasının başlanğıcıdır. Müxtəlif dalğa uzunluqlarının FSII- xlorofilin spin polyarlaşmış triplet vəziyyətində (^3Xl) Tyr_Z və Tyr_D oksidləşmə prosesindəki müxtəlifliyinin öyrənilməsi məqsədi ilə ilkin fotokimyəvi reaksiyalarına təsiri məlumat əldə etmək üçün məlumat kimi götürülmüşdür.

Nəticələr göstərdi ki, uzun dalğalı qırmızı işığın (732nm) enerjisinin verilməsi zamanı, ilkin elektron dəlikləri Xl_{D1},aşağı enerjiyə malik olduğu güman olunan tələlərdə lokallaşır. Halbuki, qısa dalğalı (532 nm) Xl molekulları arasında P_{680} də delokallaşır.

Bütün oksidləşmə-reduksiya kofaktorları FSII ardıcıllığa malikdir ki, suyun oksidləşməsini həyata keçirməklə yanaşı, sistemi zədələyə bilən aralıq məhsullardan da qoruya bilsinlər. Məqalədə V PSII uzaqlaşmış donor-akseptor sahəsinin Tyr_Z ilə qarşılıqlı təsiri öz əksini tapmışdır. Tyr_Z və ikincili xinon akseptoru olan Q_B-nun membran arası qarşılıqlı təsiri flaşla iduksiyaolunmuş füoressensiya və EPR spektroskopiya metodu ilə öyrənilmişdir. Belə nəticəyə gəlinmişdir ki, I) Tyr_Z

oksidləşməsı Q_B-saytda hansı miqyaslı sahədə yerləşməsindən asılı olur. II) Q_B saytın modifikası xarici xinonlar hesabına zülal tərkibinin dəyişməsinə səbəb olur, hansı ki öz növbəsində Tyr_Z-His_Z hidrogen rabitəsinin təsirini dəyişdirir.

FSII kompleksi 30-dan çox zülal subvahidlərindən ibarətdir. Bitkilər və yosunlarda bunlardan dördü periferik zülal subvahidləridir (PsbO, PsbP, PsbQ və PsbTn). SOK örtən üç subvahidin, məhz PsbO, PsbP, PsbQ olması, FSII fəaliyyəti üçün vacibdir. Lakin dördüncü periferik subvahidin, PsbTn, fuksiyası hələ də məlum deyil. Məqalə VI Tyr_D oksidləşmə/redkusiyasında PsbTn rolu əvəzedici mutagenez və EPR spektroskopiya metodları ilə öyrənilmişdir. Məlum olmuşdur ki, PsbTn, zülalının olmaması Tyr_D oksidləşmə kinetikasının zədələnməsinə səbəb olur. Maraqlıdır ki, Tyr_D stabilliyinə də təsir edir. PsbTn zülalının Tyr_D proton daşınması mexanizmində iştirakı təklif olundu.

Acknowledgements

What you are reading is a piece of my life, a trip that started years ago and whose final destination is in these pages. It is a trip that I couldn't have travelled by myself. Many people contributed to my study, and generally to my life in Sweden during these years. I'll try my best to mention all, but I'm sure to miss some; please excuse me if I have not mentioned some of you.

First, I would like to sincerely thank my supervisors **Fikret Mamedov** and **Stenbjorm Styring** for their continuous support and guidance throughout my PhD study. Thank you a lot Fikret for teaching me so many things and always being so positive. I would like to thank a lot Stenbjorn for letting me grow in such a tough scientific atmosphere. I still dream about controls. You taught me to do a lot of controls, and it greatly frustrated me at the beginning but now I am really thankful to you.

I would like to thank my supervisor back in my home country **Ralphreed Gasanov** for his support and motivation during my master degree. Without you, I would not be in science or now on the way of getting my PhD degree. Thank you for all atmosphere you brought to our department.

I would like to express my sincere gratitude to **Lene Hau** for a wonderful experience in her lab at Harvard and for all inspirational scientific discussions we had!

My many thanks go to **Johannes Sjöholm** for sharing with me a miserable life in a cold room making shots from spinach and Chlamy and helping me with all kinds of things in the lab, including the translation of the summary of my thesis to Swedish. Thanks to **Fredrik Mokvist** for creating a positive atmosphere in our office. I missed you guys, you have left me alone!

I would like to thank my friends **Nastya** and **Bagmi** for so much fun together. Thank you Nastya for listening all my complains about my

projects. Bagmi: thank you so much for everything, for taking all the best photograps of mine that I ever had, and for teaching me to be patient.

My many thanks to my life friends **Daniel** and **Mr Gio**. Both of you, **Andrea** and I were the best travelling group. Thanks Gio for motivating us for the trip to Copenhagen. Thank you Daniel for driving us down there; one of my best memories is of you driving around a roundabout while Andrea was searching for the route. Andrea thanks for organizing everything, from hotel booking to the road rutes while Daniel was driving, and for waking us up in the train on the way back from Copenhagen ... we have so many memories together.

My special thanks to my dear *docka* **Brigi**. Thank you dear for your snails, luciabullar, brownies etc. For your unpredictability. I always know that I have someone to call even in the middle of night. I would like to thank **Sankara** for a nice two years in our group. Thank you for your positive attitude. At the time of writing these acknowledgements it is the first day without you in our office but I do not have a feeling that you left, I believe that you will come back soon.

My special thanks to **Ping Huang** for teaching me EPR spectroscopy. Thank you a lot for organizing very interesting classes. You motivated me to study Quantum mechanics which was beyond my understanding before. Thank you a lot for helping me to get my passport from a post office otherwise I could not have been able to attend an amazing summer school and a conference in Boston.

My many thanks to the past and present coworkers in the Photosynthesis and Cyano groups: **Ann Magnuson, Felix Ho, Patricia Raleiras, Julien Jacques, Miguel Keijzers, Long Vo Pham, Johan Pettersson, Mun Hon Cheah, Karin Stensjö, Pia Lindberg, Peter Lindblad** - for our interactions and discussions every day. To **Livia Meszaros** for letting me to play with your lovely son and for being a nice neigbour in Norbyvägen. To **Charlene Esmieu** for nice morning chats. To **Gustav Bergren** for your friendly personality.... I am sure nobody will notice it ☺ except you and Fikret.

My warmest thank to **Leif Hammarström** and **Jan Davidsson** for taking care of our department.

My special thanks to **Elias Englund, Claudia Durall, Rui Miao, Feiyan Liang, Adam Wegelius,** and **Namita Khanna** for your hospitality during my first years. I always say you guys adopted me to your group. Thanks for all the amazing parties you arranged.

My many thanks to **Susanne Söderberg**. Thank you a lot Susanne for all your administrative help. You are one of the people in our department with whom I could share many things.

It has been a long list but I can not forget about the chemistry guys downstairs. Thank you to everyone in that corridor. My many thanks to **Michele Bedin, Keyhan Esfandiarfard, Juri Mai** for the nice chats we had from time to time during lunch time.

It is time to thank my friends outside of academia. My life friends from USA: **Tim Way, Cesar Zavala and Jayson de Vera** for the amazing summer school experience in Harvard. Thank you very much to you, Tim, and to your wife **Ramona** for reading my thesis. I hope you enjoyed it! You helped me a lot throughout my stressful time. Cesar and Jayson: thank you for making my summer in Boston unforgetable. All my best US memories are related to you! Thank you Cesar for all your stories dedicated to me during summer school, I still have them ☺. Thank you Jayson for arranging trip to the Niagara falls, it was the best birthday gift!

My friends from Baku, **Cahana** and **Medina**, my private psychologists ☺ throughout the long dark Swedish winter. If someone ask me how to survive long dark periods of Sweden my first advice would be to have friends who never let you feel depressed, that are always there to help you. I was lucky to get to know you.

My special thanks to **Faik**. Words are not enough to express how I am grateful to you for all the best times we had together. You showed me a different side of Sweden. Thank you for always being there for me.

I would like to thank **Lala Mamedova** for translating the summary of my thesis to Azeri. Thank you a lot for a great translation! My gratitude for the cover drawing to **Racab Muslumov**.

My Family!!! My **dad** and **mom** you are the reason of all achievments in my life. Without your support and the inspiration that you gave me, my dreams would never could come true. Thank you for being the best parents. My brothers **Vusal** and **Orkhan**, you are everything to me! And my sister and friend **Maltam** for all your positive attitude which you brought to our family. I am looking forward to meet my nephew who decided to come to our world exactly during my defense time. Thank you for being my special present!

Finally, my gratitude to the **State Oil Fund of Azerbaijan** and to the **Ministry of Education of Azerbaijan** for their help on making my dream to come true through a PhD studies research stipend.

References

[1] X. Wei, X. Su, P. Cao, X. Liu, W. Chang, M. Li, X. Zhang, Z. Liu, Structure of spinach photosystem II–LHCII supercomplex at 3.2 Å resolution, Nature, 534 (2016) 69-74.

[2] T. Cardona, A fresh look at the evolution and diversification of photochemical reaction centers, Photosyn. Res., 126 (2015) 111-134.

[3] J. Barber, 'Photosystem II: the water splitting enzyme of photosynthesis and the origin of oxygen in our atmosphere', Quart. Rev. Biophys., 49 (2016) 1-20.

[4] U.S.E.I. Administration, International Energy Outlook 2016, (2016).

[5] N.S. Lewis, D.G. Nocera, Powering the planet: Chemical challenges in solar energy utilization, Proc. Nat. Acad. Sci. U. S. A., 103 (2006) 15729-15735.

[6] M.I. Hoffert, K. Caldeira, A.K. Jain, E.F. Haites, L.D.D. Harvey, S.D. Potter, M.E. Schlesinger, S.H. Schneider, R.G. Watts, T.M.L. Wigley, D.J. Wuebbles, Energy implications of future stabilization of atmospheric CO2 content, Nature, 395 (1998) 881-884.

[7] B.S. Review, BP Statistical Review of World Energy June 2016 bp.com/statisticalreview, (2016).

[8] U.N.D. Program, World energy assessment report: energy and the challenge of sustainability, New York, NY: United Nations, (2003).

[9] I.E. Agency, CO2 emission from fuel combustion, (2016).

[10] R.A. Pachauri R, Contribution of working groups I, II, and III to the fourth assessment. Report of the Intergovernmental Panel on Climate Change. In Climate change 2007, synthesis report Geneva, Switzerland: IPCC, (2007).

[11] S.E.U.W. 2005, Basic science needs for solar energy utilization, Washington, DC: US Department of Energy.

[12] J. Barber, Biological solar energy, Philosophical Transactions of the Royal Society A: Mathematical, Physical and Engineering Sciences, 365 (2007) 1007.

[13] J. Barber, P.D. Tran, From natural to artificial photosynthesis, Jour. Roy. Soc. Inter., 10 (2013) 20120984.

[14] R.E. Blankenship, Molecular mechanisms of Photosynthesis, (2014).

[15] R. Hill, F.A.Y. Bendall, Function of the Two Cytochrome Components in Chloroplasts: A Working Hypothesis, Nature, 186 (1960) 136-137.

[16] L.N.M. Duysens, J. Amesz, B.M. Kamp, Two Photochemical Systems in Photosynthesis, Nature, 190 (1961) 510-511.

[17] G. Renger, T. Renger, Photosystem II: The machinery of photosynthetic water splitting, Photosyn. Res., 98 (2008) 53-80.
[18] Y. Umena, K. Kawakami, J.R. Shen, N. Kamiya, Crystal structure of oxygen-evolving photosystem II at a resolution of 1.9 angstrom, Nature, 473 (2011) 55-U65.
[19] M. Suga, F. Akita, K. Hirata, G. Ueno, H. Murakami, Y. Nakajima, T. Shimizu, K. Yamashita, M. Yamamoto, H. Ago, J.R. Shen, Native structure of photosystem II at 1.95 angstrom resolution viewed by femtosecond X-ray pulses, Nature, 517 (2015) 99-U265.
[20] L.-X. Shi, W.P. Schröder, The low molecular mass subunits of the photosynthetic supracomplex, photosystem II, Biochim. Biophys. Acta - Bioenergetics, 1608 (2004) 75-96.
[21] M. Swiatek, R.E. Regel, J. Meurer, G. Wanner, H.B. Pakrasi, I. Ohad, R.G. Herrmann, Effects of selective inactivation of individual genes for low-molecular-mass subunits on the assembly of photosystem II, as revealed by chloroplast transformation: The psbEFLJ operon in Nicotiana tabacum, Molecul. Genet. and Genom., 268 (2003) 699-710.
[22] Y. Umena, K. Kawakami, J.-R. Shen, N. Kamiya, Crystal structure of oxygen-evolving photosystem II at a resolution of 1.9[thinsp]A, Nature, 473 (2011) 55-60.
[23] F. Müh, C. Glöckner, J. Hellmich, A. Zouni, Light-induced quinone reduction in photosystem II, Biochim. Biophys. Acta - Bioenergetics, 1817 (2012) 44-65.
[24] T. Cardona, A. Sedoud, N. Cox, A.W. Rutherford, Charge separation in Photosystem II: A comparative and evolutionary overview, Biochim. Biophys. Acta - Bioenergetics, 1817 (2012) 26-43.
[25] M. Grabolle, H. Dau, Energetics of primary and secondary electron transfer in Photosystem II membrane particles of spinach revisited on basis of recombination-fluorescence measurements, Biochim. Biophys. Acta - Bioenergetics, 1708 (2005) 209-218.
[26] J. Messinger, Photosynthetic water splitting, in Primary processes of photosynthesis part 2, RSC Publishing, Cambridge, (2008) 291-349.
[27] B. Kok, Forbush, B., and McGloin, M., Cooperation of charges in photosynthetis O_2 evolution-I. A linear four step mechanism, Photochem. Photobiol., *11* (1970) 457-475.
[28] Govindjee, Photosystem II: The light-driven water: Plastoquinone oxidoreductase, edited by Thomas J. Wydrzynski and Kimiyuki Satoh, Volume 22, Advances in Photosynthesis and Respiration, Springer, Dordrecht, The Netherlands, Photosynthesis Research, 87 (2006) 331-335.
[29] D.H. Stewart, G.W. Brudvig, Cytochrome b559 of photosystem II, Biochim. Biophys. Acta - Bioenergetics, 1367 (1998) 63-87.
[30] I.L. McConnell, Substrate water binding and oxidation in photosystem II, Photosynthesis Research, 98 (2008) 261-276.
[31] J.R. Shen, The Structure of Photosystem II and the Mechanism of Water Oxidation in Photosynthesis, in: S.S. Merchant (Ed.) Ann. Rev. of Plant Biology, Vol 66, Annual Reviews, Palo Alto, 2015, pp. 23-48.

[32] P. Joliot, Period-four oscillations of the flash-induced oxygen formation in photosynthesis, in: Govindjee, J.T. Beatty, H. Gest, J.F. Allen (Eds.) Discoveries in Photosynthesis, Springer Netherlands, Dordrecht, 2005, pp. 371-378.
[33] W.F.J. Vermaas, G. Renger, G. Dohnt, The reducrion of the oxygen evolving system in chloroplasts by thylakoid components, Biochim. Biophys. Acta, 764 (1984) 194-202.
[34] G.Y. Chen, G.Y. Han, E. Goransson, F. Mamedov, S. Styring, Stability of the S3 and S2 state intermediates in Photosystem II directly probed by EPR spectroscopy, Biochemistry, 51 (2012) 138-148.
[35] S. Styring, A.W. Rutherford, In the oxygen evolving complex of Photosystem II the S0 state is oxidized to the S1 state by D+ (Signal II slow) Biochemistry, 26 (1987) 2401-2405.
[36] S. Styring, Sjöholm, J., Mamedov, F., Two tyrosines that changed the world: Interfacing the oxidizing power of photochemistry to water splitting in photosystem II, Biochim. Biophys. Acta, 1817 (2012) 76-87.
[37] B.A. Diner, R.D. Britt, The Redox-Active Tyrosines YZ and YD, in: T.J. Wydrzynski, K. Satoh, J.A. Freeman (Eds.) Photosystem II: The Light-Driven Water:Plastoquinone Oxidoreductase, Springer Netherlands, Dordrecht, 2005, pp. 207-233.
[38] P. Faller, R.J. Debus, K. Brettel, M. Sugiura, A.W. Rutherford, A. Boussac, Rapid formation of the stable tyrosyl radical in photosystem II, Proc. Natl. Acad. Sci USA, 98 (2001) 14368-14373.
[39] A.-M.A. Hays, I.R. Vassiliev, J.H. Golbeck, R.J. Debus, Role of D1-His190 in Proton-Coupled Electron Transfer Reactions in Photosystem II: A Chemical Complementation Study, Biochemistry, 37 (1998) 11352-11365.
[40] F. Mamedov, R.T. Sayre, S. Styring, Involvement of Histidine 190 on the D1 Protein in Electron/Proton Transfer Reactions on the Donor Side of Photosystem II, Biochemistry, 37 (1998) 14245-14256.
[41] H.A. Chu, A.P. Nguyen, R.J. Debus, Amino acid residues that influence the binding of manganese or calcium to Photosystem II. 1. The lumenal interhelical domains of the D1 polypeptide, Biochemistry, 34 (1995) 5839-5858.
[42] B. Svensson, I. Vass, E. Cedergren, S. Styring, Structure of donor side components in photosystem II predicted by computer modelling, The EMBO Journal, 9 (1990) 2051-2059.
[43] B. Svensson, C. Etchebest, P. Tuffery, P. vanKan, J. Smith, S. Styring, A model for the photosystem II reaction center core including the structure of the primary donor P-680, Biochemistry, 35 (1996) 14486-14502.
[44] C. Berthomieu, R. Hienerwadel, A. Boussac, J. Breton, B.A. Diner, Hydrogen bonding of redox-active tyrosine Z of photosystem II probed by FTIR difference spectroscopy, Biochemistry, 37 (1998) 10547-10554.
[45] R.J. Debus, B.A. Barry, I. Sithole, G.T. Babcock, L. McIntosh, Directed mutagenesis indicates that the donor to P680+ in Photosystem II is Tyrosine-161 of the D1 polypeptide, Biochemistry, 27 (1988) 9071-9074.
[46] K. Saito, A.W. Rutherford, H. Ishikita, Mechanism of tyrosine D oxidation in Photosystem II, Proc. Natl. Acad. Sci USA, 110 (2013) 7690-7695.

[47] I. Vass, Styring, S., pH-dependent charge equilibria between Tyrosine-D and the S states in photosystem II. Estimation of relative midpoint redox potentials, Biochemistry, 30 (1991) 830-839.
[48] K. Brettel, E. Schlodder, H.T. Witt, Nanosecond reduction kinetics of photooxidized chlorophyll-aII (P-680) in single flashes as a probe for the electron pathway, H+-release and charge accumulation in the O2-evolving complex, Biochim. Biophys. Acta - Bioenergetics, 766 (1984) 403-415.
[49] G. Christen, F. Reifarth, G. Renger, On the origin of the `35-μs kinetics' of P680+· reduction in photosystem II with an intact water oxidising complex, FEBS Lett., 429 (1998) 49-52.
[50] M.R. Razeghifard, C. Klughammer, R.J. Pace, Electron Paramagnetic Resonance Kinetic Studies of the S States in Spinach Thylakoids, Biochemistry, 36 (1997) 86-92.
[51] F. Rappaport, M. Blanchard-Desce, J. Lavergne, Kinetics of electron transfer and electrochromic change during the redox transitions of the photosynthetic oxygen-evolving complex, Biochim. Biophys. Acta (BBA) - Bioenergetics, 1184 (1994) 178-192.
[52] H.J. Eckert, G. Renger, Temperature dependence of P680+ reduction in O2-evolving PS II membrane fragments at different redox states Si of the water oxidizing system, FEBS Lett., 236 (1988) 425-431.
[53] M.J. Schilstra, F. Rappaport, J.H.A. Nugent, C.J. Barnett, D.R. Klug, Proton/Hydrogen Transfer Affects the S-State-Dependent Microsecond Phases of P680+ Reduction during Water Splitting, Biochemistry, 37 (1998) 3974-3981.
[54] G. Renger, Coupling of electron and proton transfer in oxidative water cleavage in photosynthesis, Biochim. Biophys. Acta (BBA) - Bioenergetics, 1655 (2004) 195-204.
[55] B. Meyer, E. Schlodder, J.P. Dekker, H.T. Witt, O2 evolution and ChlA II+ (P680) nanosecond reduction kinetics in single flashes as a function of pH Biochim. Biophys. Acta, 974 (1989) 36-43.
[56] R. Ahlbrink, M. Haumann, D. Cherepanov, O. Bögershausen, A. Mulkidjanian, W. Junge, Function of Tyrosine Z in Water Oxidation by Photosystem II: Electrostatical Promotor Instead of Hydrogen Abstractor, Biochemistry, 37 (1998) 1131-1142.
[57] A.W. Rutherford, A. Boussac, P. Faller, The stable tyrosyl radical in Photosystem II: why D?, Biochim. Biophys. Acta-Bioenergetics, 1655 (2004) 222-230.
[58] G.T. Babcock, K. Sauer, Electron paramagnetic resonance signal II in spinach-chloroplast .1. Kinetic analysis for untreated chloroplasts Biochim. Biophys. Acta, 325 (1973) 483-503.
[59] C.A. Buser, L.K. Thompson, B.A. Diner, G.W. Brudvig, Electron-transfer reactions in manganese-depleted photosystem II, Biochemistry, 29 (1990) 8977-8985.
[60] A. Boussac, A.L. Etienne, Spectral and kinetic pH-dependence of fast and slow Signal II in Tris-washed chloroplasts, FEBS Lett., 148 (1982) 113-116.

[61] B.R. Velthuys, J.W.M. Visser, Reactivation of EPR Signal II in chloroplasts treated with reduced dichlorophenol-indophenol. Evidence against a dark equilibrium between two oxidation states of oxygen evolvin system FEBS Lett., 55 (1975) 109-112.
[62] S. Styring, A.W. Rutherford, In the oxygen-evolving complex of photosystem II the S0 state is oxidized to the S1 state by D+ (signal IIslow), Biochemistry, 26 (1987) 2401-2405.
[63] A. Boussac, A.L. Etienne, Midpoint potential of signal II (slow) in Tris-washed photosystem-II particles, Biochim. Biophys. Acta - Bioenergetics, 766 (1984) 576-581.
[64] R.J. Debus, B.A. Barry, G.T. Babcock, L. McIntosh, Site-directed mutagenesis identifies a tyrosine radical involved in the photosynthetic oxygen-evolving system, Proc. Nat. Acad. Sci. U. S. A., 85 (1988) 427-430.
[65] S.V. Ruffle, D. Donnelly, T.L. Blundell, J.H.A. Nugent,
A 3-dimensional model of the Photosystem II reaction center of *Pisum Sativum*, Photosyn. Res., 34 (1992) 287-300.
[66] K.A. Campbell, J.M. Peloquin, B.A. Diner, X.-S. Tang, D.A. Chisholm, R.D. Britt, The τ-Nitrogen of D2 Histidine 189 is the Hydrogen Bond Donor to the Tyrosine Radical YD• of Photosystem II, Jour. Am. Chem. Soc., 119 (1997) 4787-4788.
[67] C. Tommos, L. Davidsson, B. Svensson, C. Madsen, W. Vermaas, S. Styring, Modified EPR spectra of the tyrosineD radical in photosystem II in site-directed mutants of Synechocystis sp. PCC 6803: Identification of side chains in the immediate vicinity of tyrosineD on the D2 protein, Biochemistry, 32 (1993) 5436-5441.
[68] W.F.J. Vermass, A.W. Rutherford, Ö. Hansson, Site-directed mutagenesis in photosystem II of the cyanobacterium Synechocystis sp. PCC 6803: Donor D is a tyrosine residue in the D2 protein, Proceedings of the National Academy of Sciences, 85 (1988) 8477-8481.
[69] C. Jeans, M.J. Schilstra, N. Ray, S. Husain, J. Minagawa, J.H.A. Nugent, D.R. Klug, Replacement of Tyrosine D with Phenylalanine Affects the Normal Proton Transfer Pathways for the Reduction of P680+ in Oxygen-Evolving Photosystem II Particles from Chlamydomonas, Biochemistry, 41 (2002) 15754-15761.
[70] R.J. Boerner, K.A. Bixby, A.P. Nguyen, G.H. Noren, R.J. Debus, B.A. Barry, Removal of stable tyrosine radical D+ affects the structure or redox properties of tyrosine Z in manganese-depleted photosystem II particles from Synechocystis 6803, Journal of Biological Chemistry, 268 (1993) 1817-1823.

[71] B.A. Diner, E. Schlodder, P.J. Nixon, W.J. Coleman, F. Rappaport, J. Lavergne, W.F.J. Vermaas, D.A. Chisholm, Site-Directed Mutations at D1-His198 and D2-His197 of Photosystem II in Synechocystis PCC 6803: Sites of Primary Charge Separation and Cation and Triplet Stabilization, Biochemistry, 40 (2001) 9265-9281.
[72] K.G.V. Havelius, S. Styring, pH dependent competition between YZ and YD in photosystem II probed by illumination at 5 K, Biochemistry, 46 (2007) 7865-7874.
[73] F.J. Ruzicka, H. Beinert, K.L. Schepler, W.R. Dunham, R.H. Sands, Interaction of ubisemiquinone with a paramagnetic component in heart tissue, Proc. Nat. Acad. Sci. U. S. A., 72 (1975) 2886-2890.
[74] G. Zahariou, M. Chrysina, V. Petrouleas, N. Ioannidis, Can we trap the S3YZ center dot Z metalloradical intermediate during the S-state transitions of Photosystem II? An EPR investigation, FEBS Lett., 588 (2014) 1827-1831.
[75] N. Ioannidis, G. Zahariou, V. Petrouleas, The EPR spectrum of tyrosine Z(center dot) and its decay kinetics in O(2)-evolving photosystem II preparations, Biochemistry, 47 (2008) 6292-6300.
[76] B. Commoner, J.J. Heise, J. Townsend, Light induced paramagnetism in chloroplasts, Proc. Nat. Acad. Sci. U. S. A., 42 (1956) 710-718.
[77] G.T. Babcock, K. Sauer, A rapid, light-induced transient in electron paramagnetic resonance signal II activated upon inhibition of photosynthetic oxygen evolution, Biochim. Biophys. Acta - Bioenergetics, 376 (1975) 315-328.
[78] G. T. Babcock, R. E. Blankenship, K. Sauer, Reaction kinetics for positive charge accumulation on the water side of choloplast photosystem II, FEBS Lett., 61 (1976) 286-289.
[79] G.C. Dismukes, Y. Siderer, Intermediates of a polynuclear manganese center involved in photosynthetic oxidation of water, Proc. Nat. Acad. Sci. U. S. A., 78 (1981) 274-278.
[80] A.W. Rutherford, J.L. Zimmermann, A New Electron Paramagnetic Resonance Signal Attributed to the Primary Plastosemiquinone Acceptor in Photosystem II, Biochim. Biophys. Acta, 767 (1984) 168-175.
[81] A. Sedoud, N. Cox, M. Sugiura, W. Lubitz, A. Boussac, A.W. Rutherford, Semiquinone–Iron Complex of Photosystem II: EPR Signals Assigned to the Low-Field Edge of the Ground State Doublet of QA•–Fe2+ and QB•–Fe2+, Biochemistry, 50 (2011) 6012-6021.
[82] W.O. Feikema, P. Gast, I.B. Klenina, I.I. Proskuryakov, EPR characterisation of the triplet state in photosystem II reaction centers with singly reduced primary acceptor QA, Biochim. Biophys. Acta - Bioenergetics, 1709 (2005) 105-112.
[83] K. Maxwell, G.N. Johnson, Chlorophyll fluorescence — a practical guide, Jour. Experim. Botany, 51 (2000) 659-668.

[84] F.L. Figueroa, C.G. Jerez, N. Korbee, Use of in vivo chlorophyll fluorescence to estimate photosynthetic activity and biomass productivity in microalgae grown in different culture systems, Lat. Am. J. Aquat. Res., 41 (2013) 801-819.
[85] N.R. Baker, Chlorophyll fluorescence: A probe of photosynthesis in vivo, in: Annu. Rev. Plant Biol., Annual Reviews, Palo Alto, 2008, pp. 89-113.
[86] H. Kautsky, W. Appel, H. Amann, Chlorophyll fluorescenz und kohlensaure assimilation 13. Die fluorescenz kurve und die photochemie der pflanze, Biochemische Zeitschrift, 332 (1960) 277-292.
[87] G.H. Krause, E. Weis, Chlorophyll fluorescence and photosynthesis - The basics, Annu. Rev. Plant Physiol. Plant Molec. Biol., 42 (1991) 313-349.
[88] G. Renger, H.J. Eckert, A. Bergmann, J. Bernarding, B. Liu, A. Napiwotzki, F. Reifarth, H.J. Eichler, Fluorescence and spectroscopic studies of exciton trapping and electron transfer in Photosystem II of higher plants, Aust. J. Plant Physiol., 22 (1995) 167-181.
[89] I. Vass, D. Kirilovsky, A.L. Etienne, UV-B radiation-induced donor- and acceptor-side modifications of photosystem II in the cyanobacterium Synechocystis sp PCC 6803, Biochemistry, 38 (1999) 12786-12794.
[90] F. Mamedov, H. Stefansson, P.A. Albertsson, S. Styring, Photosystem II in different parts of the thylakoid membrane: A functional comparison between different domains, Biochemistry, 39 (2000) 10478-10486.
[91] F. Mamedov, M.M. Nowaczyk, A. Thapper, M. Rogner, S. Styring, Functional characterization of monomeric photosystem II core preparations from Thermosynechococcus elongatus with or without the Psb27 protein, Biochemistry, 46 (2007) 5542-5551.
[92] M. Rova, F. Mamedov, A. Magnuson, P.O. Fredriksson, S. Styring, Coupled activation of the donor and the acceptor side of photosystem II during photoactivation of the oxygen evolving cluster, Biochemistry, 37 (1998) 11039-11045.
[93] W. Arnold, J. Thompson, Delayed light production by blue green algae, red algae and purple bacteria, Jour. of Gen.Phys., 39 (1956) 311-318.
[94] I. Vass, Govindjee, Thermoluminescence from the photosynthetic apparatus, Photosyn. Res., 48 (1996) 117-126.
[95] F. Rappaport, J. Lavergne, Thermoluminescence: theory, Photosynthesis Research, 101 (2009) 205-216.
[96] S.Y. Reece, D.G. Nocera, Proton-Coupled Electron Transfer in Biology: Results from Synergistic Studies in Natural and Model Systems, Annual review of biochemistry, 78 (2009) 673-699.
[97] A. Migliore, N.F. Polizzi, M.J. Therien, D.N. Beratan, Biochemistry and Theory of Proton-Coupled Electron Transfer, Chemical Reviews, 114 (2014) 3381-3465.
[98] S. Nakamura, T. Noguchi, Infrared detection of a proton released from Tyrosine YD to the bulk upon its photo-oxidation in Photosystem II, Biochemistry, 54 (2015) 5045-5053.

[99] A. Thapper, F. Mamedov, F. Mokvist, L. Hammarström, S. Styring, Defining the Far-Red Limit of Photosystem II in Spinach, The Plant Cell, 21 (2009) 2391-2401.
[100] F. Mokvist, J. Sjöholm, F. Mamedov, S. Styring, The Photochemistry in Photosystem II at 5 K Is Different in Visible and Far-Red Light, Biochemistry, 53 (2014) 4228-4238.
[101] J.L. Hughes, P. Smith, R. Pace, E. Krausz, Charge separation in photosystem II core complexes induced by 690–730 nm excitation at 1.7 K, Biochim. Biophys. Acta - Bioenergetics, 1757 (2006) 841-851.
[102] E. Romero, Bruce A. Diner, Peter J. Nixon, Wiliam J. Coleman, Jan P. Dekker, R. van Grondelle, Mixed Exciton–Charge-Transfer States in Photosystem II: Stark Spectroscopy on Site-Directed Mutants, Biophys. Journal, 103 (2012) 185-194.
[103] E. Romero, I.H.M. van Stokkum, V.I. Novoderezhkin, J.P. Dekker, R. van Grondelle, Two Different Charge Separation Pathways in Photosystem II, Biochemistry, 49 (2010) 4300-4307.
[104] V.I. Novoderezhkin, R. Croce, M. Wahadoszamen, I. Polukhina, E. Romero, R. van Grondelle, Mixing of exciton and charge-transfer states in light-harvesting complex Lhca4, Phys. Chem. Chem. Phys., 18 (2016) 19368-19377.
[105] G. Raszewski, W. Saenger, T. Renger, Theory of Optical Spectra of Photosystem II Reaction Centers: Location of the Triplet State and the Identity of the Primary Electron Donor, Biophys. Jour., 88 (2005) 986-998.
[106] B.A. Diner, F. Rappaport, Structure, dynamics, and energetics of the primary photochemistry of photosystem II of oxygenic photosynthesis, An. Rev. Pl. Biol., 53 (2002) 551-580.
[107] E. Schlodder, W.J. Coleman, P.J. Nixon, R.O. Cohen, T. Renger, B.A. Diner, Site-directed mutations at D1-His198 and D1-Thr179 of photosystem II in Synechocystis sp PCC 6803: deciphering the spectral properties of the PSII reaction centre, Philosoph. Trans. Roy. Soc. B-Biol. Sci., 363 (2008) 1197-1202.
[108] N. Ohnishi, Y. Kashino, K. Satoh, Y. Takahashi, Functional characterization of PsbT in the repair of photodamaged PSII cofactors, Plant Cell Physiol., 43 (2002) S62-S62.
[109] L.X. Shi, W.P. Schroder, The low molecular mass subunits of the photosynthetic supracomplex, photosystem II, Biochim. Biophys. Acta-Bioenergetics, 1608 (2004) 75-96.
[110] Y. Chen, Lezheneva, L., Meurer, J., Schwenker, S., Mamedov, F., Schröder, W., The low molecular mass PsbTn protein in Photsystem II of Arabidopsis plant, manuscript.
[111] U. Ljungberg, H.E. Akerlund, B. Andersson, Isolation and characterization of the 10-kDa and 22 kDa polypeptides of higher plant Photosystem II, Europ. Jour. Biochem., 158 (1986) 477-482.
[112] M. Ikeuchi, K. Takio, Y. Inoue, N-terminal sequencing of Photosystem II low molecular mass proteins - 5 and 4.1 kDa components of the O2 evolving complex from higher plants, FEBS Lett., 242 (1989) 263-269.

[113] N. Ahmadova, F.M. Ho, S. Styring, F. Mamedov, Tyrozine D oxidation and redox equilibrium in photosystem II, Biochim. Biophys. Acta - Bioenergetics, 1858 (2017) 407-417.
[114] L.E. Andreasson, I. Vass, S. Styring, Ca2+ depletion modifies the electron transfer on both donor and acceptor side in Photosystem II from spinach, Biochim. Biophys. Acta-Bioenergetics, 1230 (1995) 155-164.
[115] J. Sjöholm, F. Ho, N. Ahmadova, K. Brinkert, L. Hammarström, F. Mamedov, S. Styring, The protonation state around TyrD/TyrD• in photosystem II is reflected in its biphasic oxidation kinetics, Biochim. Biophys. Acta - Bioenergetics, 1858 (2017) 147-155.
[116] Y. Kato, T. Noguchi, Long-Range Interaction between the Mn4CaO5 Cluster and the Non-heme Iron Center in Photosystem II as Revealed by FTIR Spectroelectrochemistry, Biochemistry, 53 (2014) 4914-4923.
[117] A. Krieger, E. Weis, Energy dependent quenching of chlrophyll A fluorescence. The involvement of proton calcium exchange at Photosystem II, Photosynthetica, 27 (1992) 89-98.
[118] S.I. Allakhverdiev, T. Tsuchiya, K. Watabe, A. Kojima, D.A. Los, T. Tomo, V.V. Klimov, M. Mimuro, Redox potentials of primary electron acceptor quinone molecule (Q(A))(−) and conserved energetics of photosystem II in cyanobacteria with chlorophyll a and chlorophyll d, Proc. Nat. Acad. Sci. U. S. A., 108 (2011) 8054-8058.
[119] G.N. Johnson, A.W. Rutherford, A. Krieger, A change in the midpoint potential of the quinone QA in Photosystem II associated with photoactivation of oxygen evolution, Biochim. Biophys. Acta - Bioenergetics, 1229 (1995) 202-207.
[120] K. Ido, C.M. Gross, F. Guerrero, A. Sedoud, T.-L. Lai, K. Ifuku, A. William Rutherford, A. Krieger-Liszkay, High and low potential forms of the QA quinone electron acceptor in Photosystem II of Thermosynechococcus elongatus and spinach, Jour. Photochem. and Photobiol. B: Biol., 104 (2011) 154-157.
[121] A. Krieger-Liszkay, A.W. Rutherford, Influence of Herbicide Binding on the Redox Potential of the Quinone Acceptor in Photosystem II: Relevance to Photodamage and Phytotoxicity, Biochemistry, 37 (1998) 17339-17344.
[122] A.W. Rutherford, A. Krieger-Liszkay, Herbicide-induced oxidative stress in photosystem II, Trends in Biochemical Sciences, 26 (2001) 648-653.
[123] M. Broser, C. Glöckner, A. Gabdulkhakov, A. Guskov, J. Buchta, J. Kern, F. Müh, H. Dau, W. Saenger, A. Zouni, Structural Basis of Cyanobacterial Photosystem II Inhibition by the Herbicide Terbutryn, The Jour. Biol. Chem., 286 (2011) 15964-15972.
[124] M. Jackson, H.H. Mantsch, Beware of proteins in DMSO, Biochim. Biophys. Acta - Protein Structure and Molecular Enzymology, 1078 (1991) 231-235.

Acta Universitatis Upsaliensis

Digital Comprehensive Summaries of Uppsala Dissertations from the Faculty of Science and Technology 1527

Editor: The Dean of the Faculty of Science and Technology

A doctoral dissertation from the Faculty of Science and Technology, Uppsala University, is usually a summary of a number of papers. A few copies of the complete dissertation are kept at major Swedish research libraries, while the summary alone is distributed internationally through the series Digital Comprehensive Summaries of Uppsala Dissertations from the Faculty of Science and Technology. (Prior to January, 2005, the series was published under the title "Comprehensive Summaries of Uppsala Dissertations from the Faculty of Science and Technology".)

Distribution: publications.uu.se
urn:nbn:se:uu:diva-320916

ACTA
UNIVERSITATIS
UPSALIENSIS
UPPSALA
2017